In vivo characterization of biological tissue using pulsed photothermal radiometry (PPTR)

Boris Majaron

Jožef Stefan Institute, Ljubljana, Slovenia

Faculty of Mathematics and Physics, University of Ljubljana, Slovenia

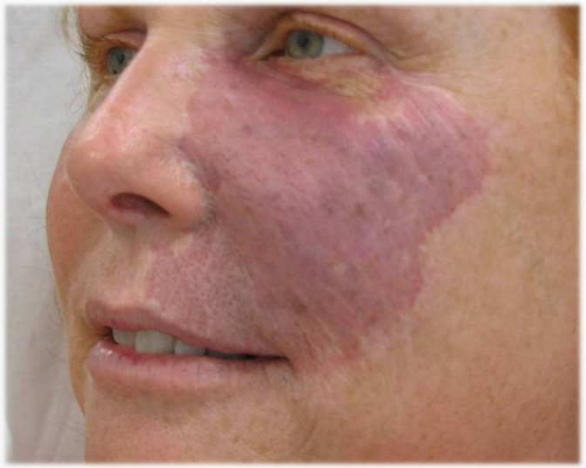

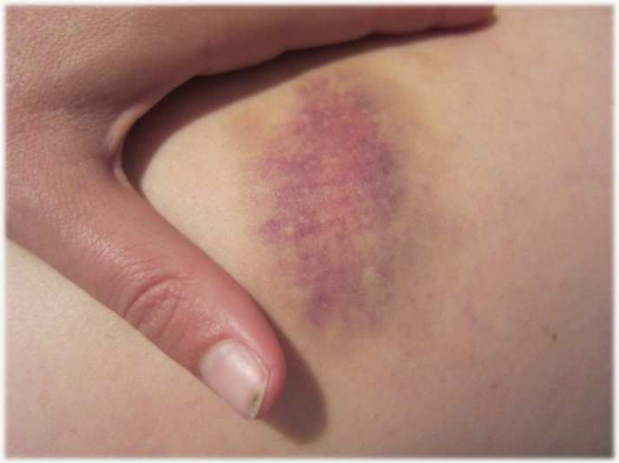

boris.majaron@ijs.si ; http://www-f7.ijs.si/en

Outline

Introduction

- theoretical foundations
- application principles

1. Specifics of biomedical applications

- spectral variation of the IR absorption coefficient

2. *In vivo* applications: Temperature depth profiling

- monitoring of laser tatoo removal
- structural characterization of vascular lesions
- response of a port-wine stain lesion to laser treatment
- Nd:YAP laser (1342 nm) energy deposition in skin
- assessment of the maximal safe radiant exposure

3. *In vivo* applications: Model-based inverse analysis

- assessment of structure and composition of human skin
- analysis of hemoglobin dynamics in traumatic bruises
- combining photothermal radiometry with optical spectroscsopy

Pulsed photo-thermal radiometry (PPTR)

1. Pulsed irradiation establishes a temperature depth profile, which then evolves with time:

$$\Delta T(z,t) = \int_{z'=0}^{\infty} \Delta T(z',t=0)\, G_{\mathrm{T}}(z',z,t)\, \mathrm{d}z'$$

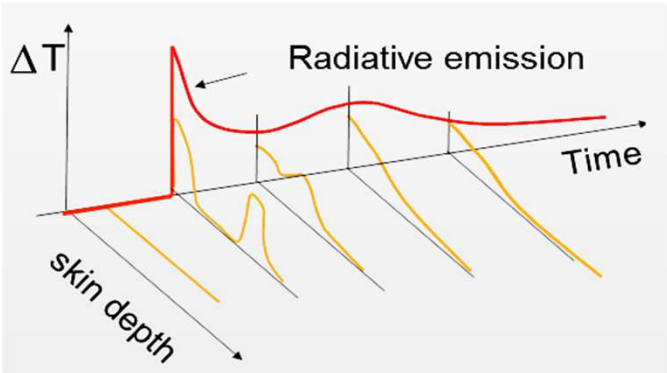

2. Transient increase in IR emission:

$$\Delta S_{\lambda}(t) = C\, \mu_{\mathrm{IR}}\, B_{\lambda}'(T_{\mathrm{b}}) \int_{z=0}^{\infty} \Delta T(z,t)\, e^{-\mu_{\mathrm{IR}} z}\, \mathrm{d}z$$

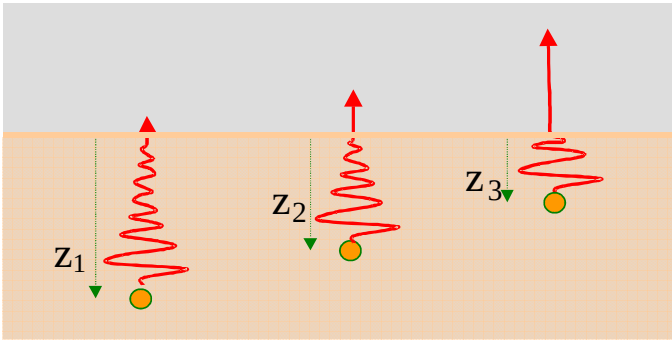

3. Leading to enclosed expression for the radiometric transient:

$$\Delta S_{\lambda}(t) = C\, \mu_{\mathrm{IR}}\, B_{\lambda}'(T_{\mathrm{b}}) \int_{z=0}^{\infty} \Delta T_0(z') \int_{z'=0}^{\infty} G_{\mathrm{T}}(z',z,t)\, e^{-\mu_{\mathrm{IR}} z}\, \mathrm{d}z\, \mathrm{d}z'$$

Milner et al., J. Opt. Soc. Am. A 12, 1479 (1995); Majaron et al., Phys. Med. Biol. 47, 1929 (2002)

PPTR application principles

$$\Delta S_\lambda(t) = C\,\mu_{IR}\,B'_\lambda(T_b)\int_{z=0}^{\infty}\Delta T_0(z)\int_{z'=0}^{\infty}G_T(z,z',t)\,e^{-\mu_{IR}z'}\,dz'\,dz$$

1.) Controlled $\Delta T_0(z)$ and IR penetration depth → **Assess thermal properties**

- standard approach for material characterization (D_T = "flash technique")
- applicable to layered structures, e.g., films on substrates)

Long et al., Appl. Phys. Lett. 51, 2076 (1987)

2.) Controlled $\Delta T_0(z)$ and thermal properties → **Determine $\mu_{IR}(\lambda)$**

3.) Controlled thermal properties and IR penetration depth → **Assess $\Delta T_0(z)$**

- a.k.a. **temperature depth profiling**
- **model-based analysis**
  (e.g., assessment of absorption and scattering coefficients in biological tissue)

Prahl et al., Phys. Med. Biol. 37, 1203 (1992)

PPTR temperature profiling *in vivo*

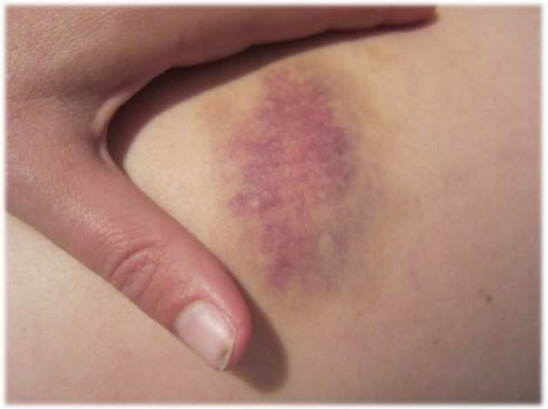

Radiometric transient

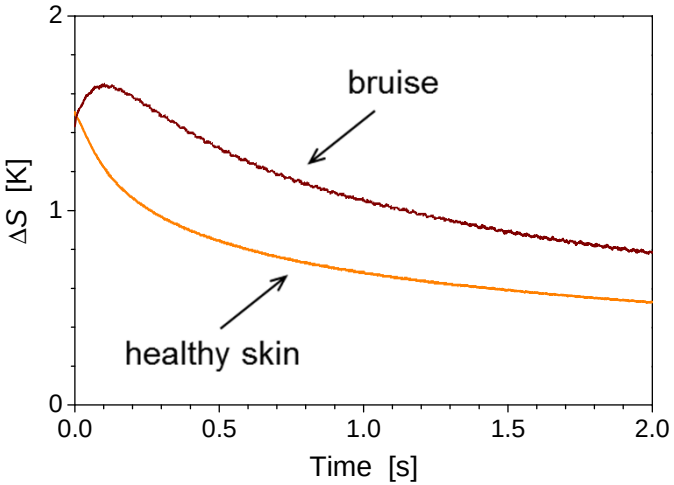

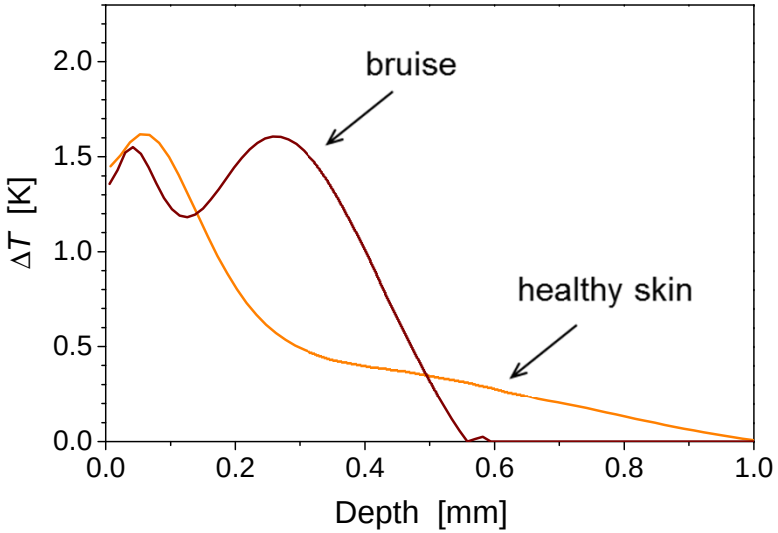

Inverse problem

of heat diffusion + radiation

Reconstructed temperature depth profiles
- in healthy vs. damaged skin

Vidovič et al., Proc. SPIE 8941, 894112 (2014)

1 May 1993 / Vol. 32, No. 13 / APPLIED OPTICS 2439

Pulsed photothermal radiometry of port-wine-stain lesions

Steven L. Jacques, J. Stuart Nelson, William H. Wright, and Thomas E. Milner

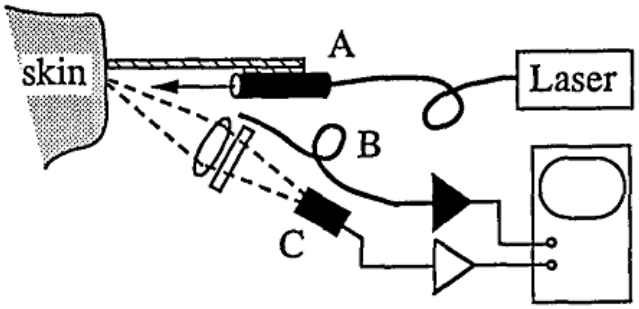

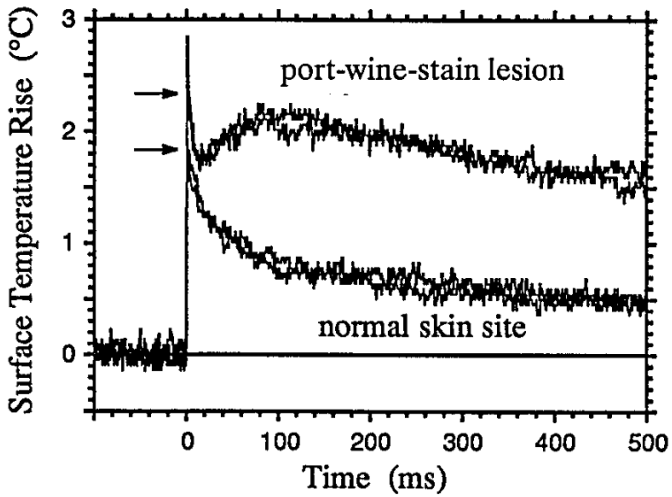

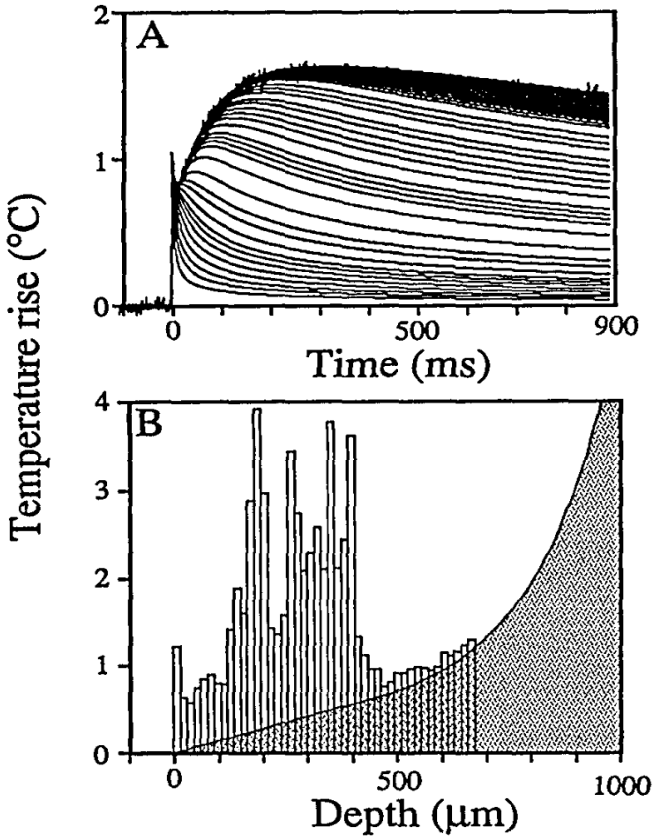

1. Heat diffusion: $\Delta T(z,t) = \int_{z'=0}^{\infty} \Delta T(z',t=0)\, \underline{G_{\mathrm{T}}(z',z,t)}\, \mathrm{d}z'$

Thermal Green's (point-spread) function:

$$G_{\mathrm{T}}(z',z,t) = \frac{1}{\sqrt{4\pi Dt}} \left\{ e^{-\frac{(z-z')^2}{4Dt}} + e^{-\frac{(z+z')^2}{4Dt}} \left[1 - h\sqrt{4\pi Dt}\, e^{u^2} erfc(u) \right] \right\}$$

where:

$erfc(u) = 1 - erf(u)$

$$u = \frac{z+z'}{2\sqrt{Dt}} + h\sqrt{Dt}$$

$D = 1.1 \times 10^{-7}\ \mathrm{m^2/s}$

$h = 0.02\ \mathrm{mm^{-1}}$

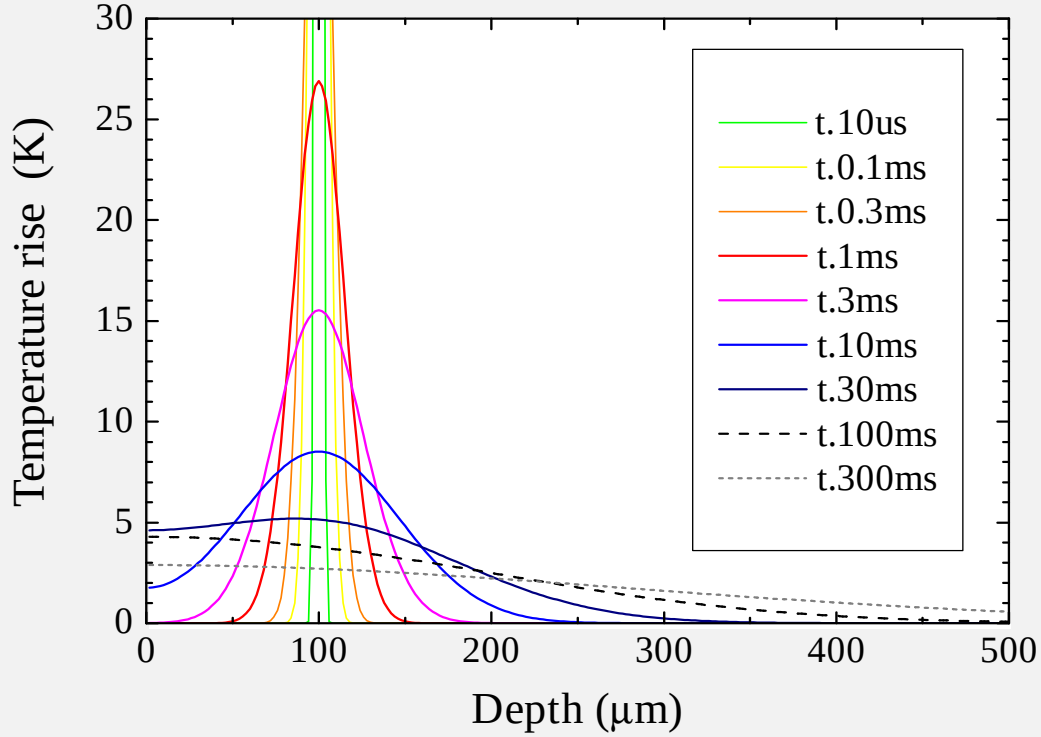

combine: $\Delta S_\lambda(t) = C\,\mu_{IR}\,B_\lambda'(T_b)\int_{z=0}^{\infty}\Delta T_0(z)\int_{z'=0}^{\infty}G_T(z,z',t)\,e^{-\mu_{IR}z'}\,dz'\,dz$

$$\Delta S_\lambda(t) = \int_{z=0}^{\infty} K(z,t)\,\Delta T_0(z)\,dz$$

Kernel function:

$$K(z',t) = \frac{1}{2}C\,B_\lambda'(T_0)\,\mu_{IR}\,e^{-\frac{z'^2}{4Dt}}\left\{erfcx(u_-) + erfcx(u_+) - \frac{2h}{(h-\mu_{IR})}\left[erfcx(u_+) - erfcx(u_1)\right]\right\}$$

where:

$$erfcx(u) = exp(u^2)\,(1 - erf(u))$$

$$u_\pm = \mu_a\sqrt{Dt} \pm \frac{z'}{2\sqrt{Dt}}$$

$$u_1 = h\sqrt{Dt} \pm \frac{z'}{2\sqrt{Dt}}$$

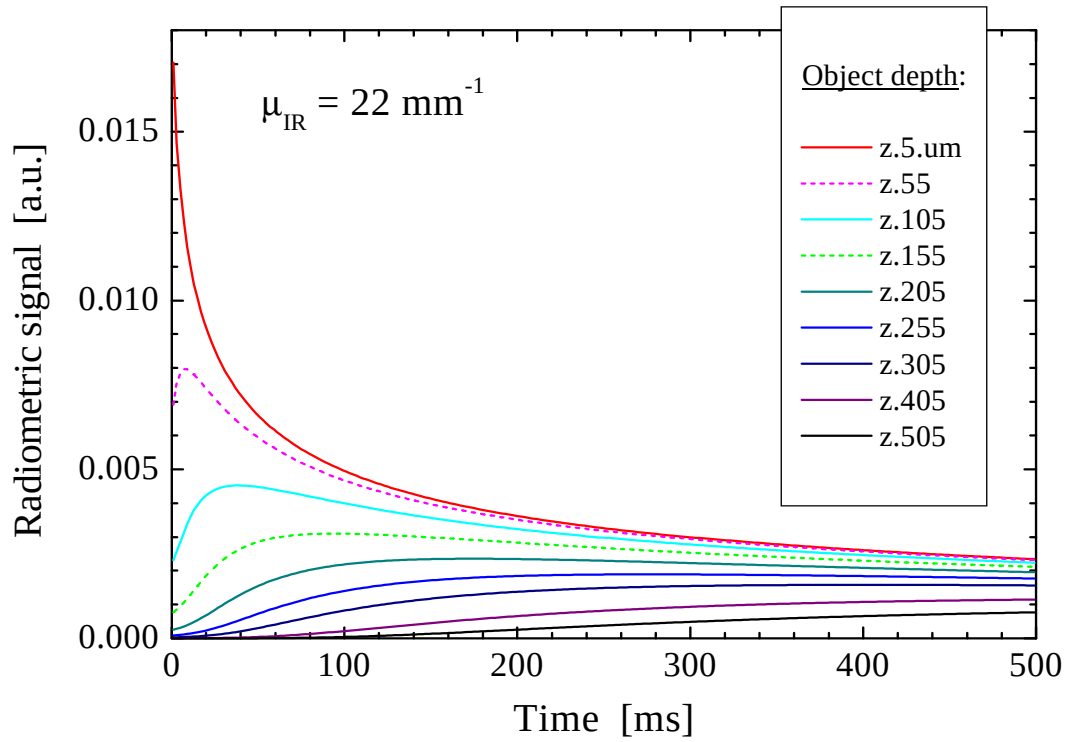

The inverse problem of PPTR profiling

Forward problem (= heat diffusion + IR emission):

$$\Delta S(t) = \int_{z=0}^{\infty} K(z,t)\, \Delta T_0(z)\, \mathrm{d}z$$

$$\boldsymbol{S} = \mathbf{K}\ \boldsymbol{T}$$

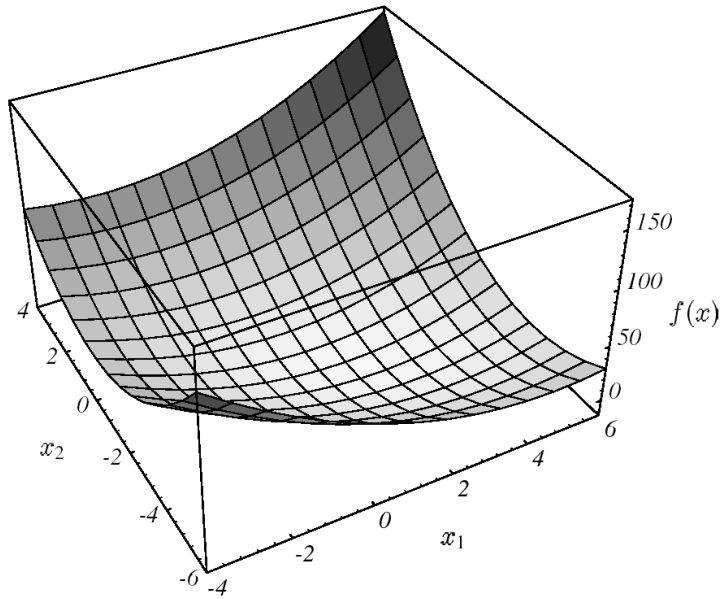

Inverse problem: $\boldsymbol{T} = \mathbf{K}^{-1}\, \boldsymbol{S}$

- matrix $\mathbf{K}$ has a defect rank - non-invertable
- inverse problem is "severely ill-posed"
- no unique solution in general

→ iterative reconstruction – multidimensional minimization of

$$\left\| \boldsymbol{r}^{(l)} \right\|^2 = \left\| \mathrm{K}\boldsymbol{T}^{(l)} - \boldsymbol{S} \right\|^2$$

1. Specifics of biomedical applications

- Excitation source
- Acquisition spectral band
- Spectral variation of the IR absorption coefficient

Selection of the excitation laser (pulsed!)

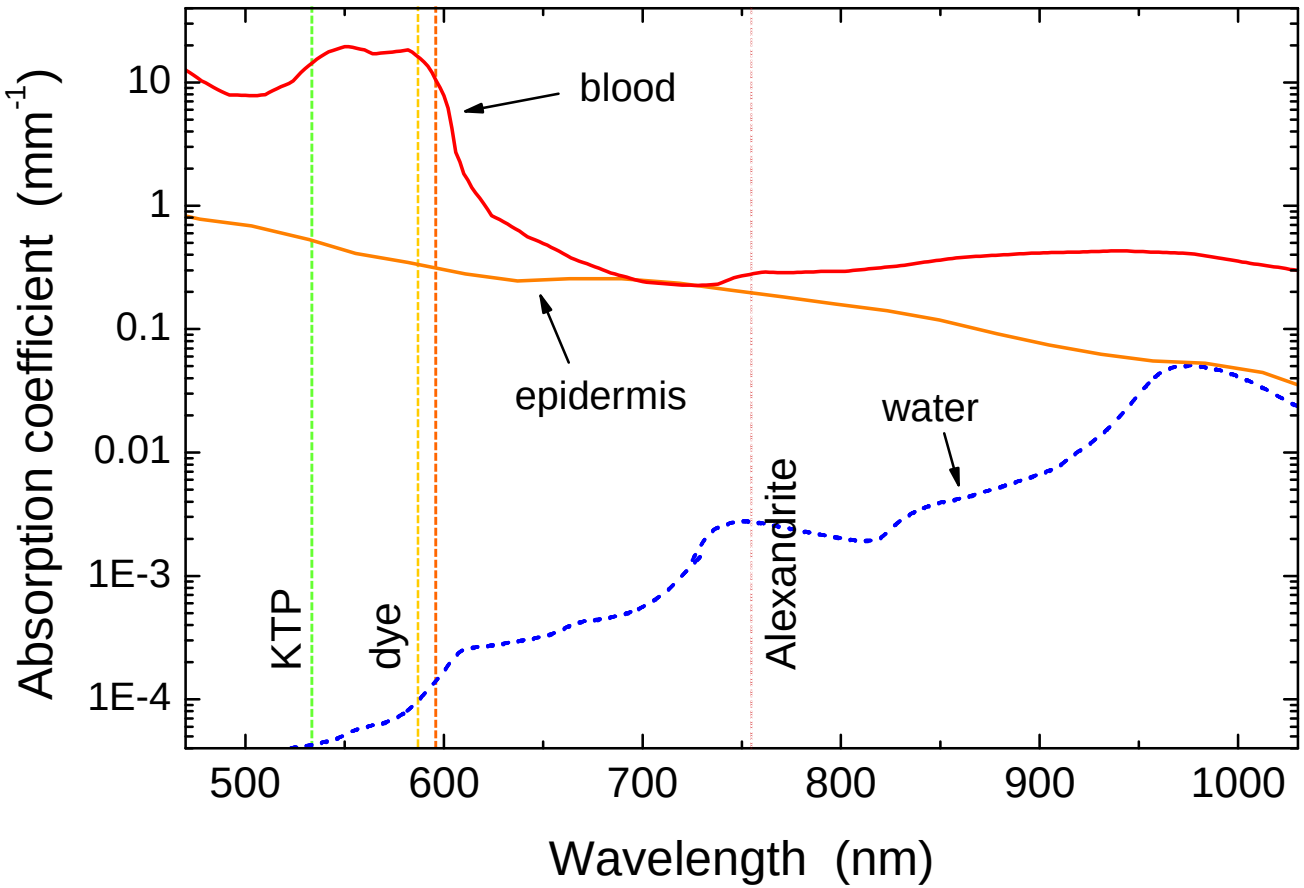

Note: You can apply PPTR with any pulsed light source !

Radiative emission:

$$\Delta S(t) = C\, B_\lambda'(T_0)\, \mu_{IR} \int_{z=0}^{\infty} \Delta T(z,t)\, e^{-\mu_{IR} z}\, dz$$

Planck's law:

$$B_\lambda(T) = \frac{2\pi h c^2}{\lambda^5} \left(e^{\frac{hc}{\lambda k T}} - 1\right)^{-1}$$

Temperature derivative:

$$B_\lambda'(T_0) = \frac{2\pi h^2 c^3}{\lambda^5 k T_0^2} \frac{e^{-\frac{hc}{\lambda k T_0}}}{\left(e^{\frac{hc}{\lambda k T_0}} - 1\right)^2}$$

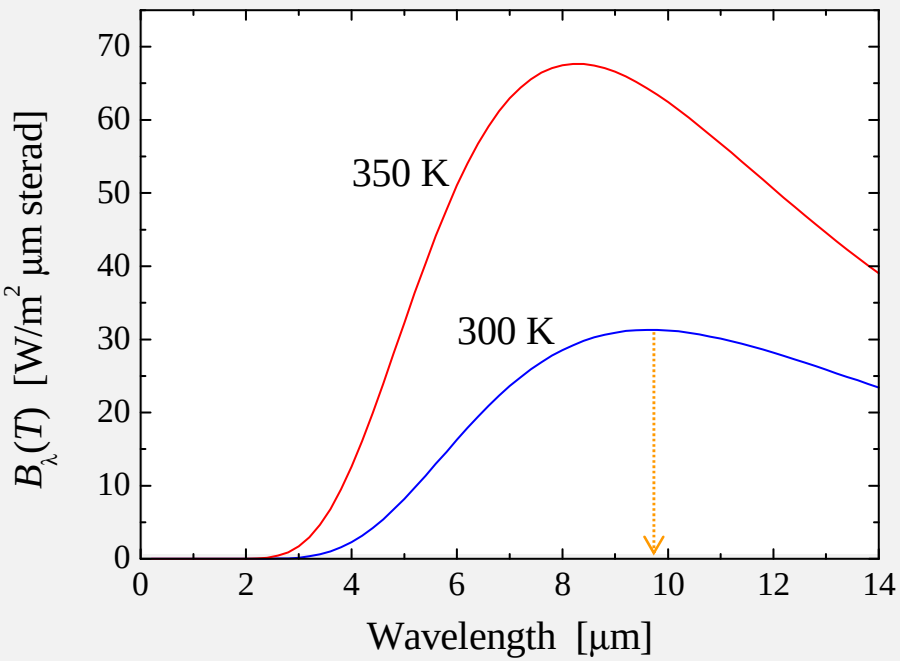

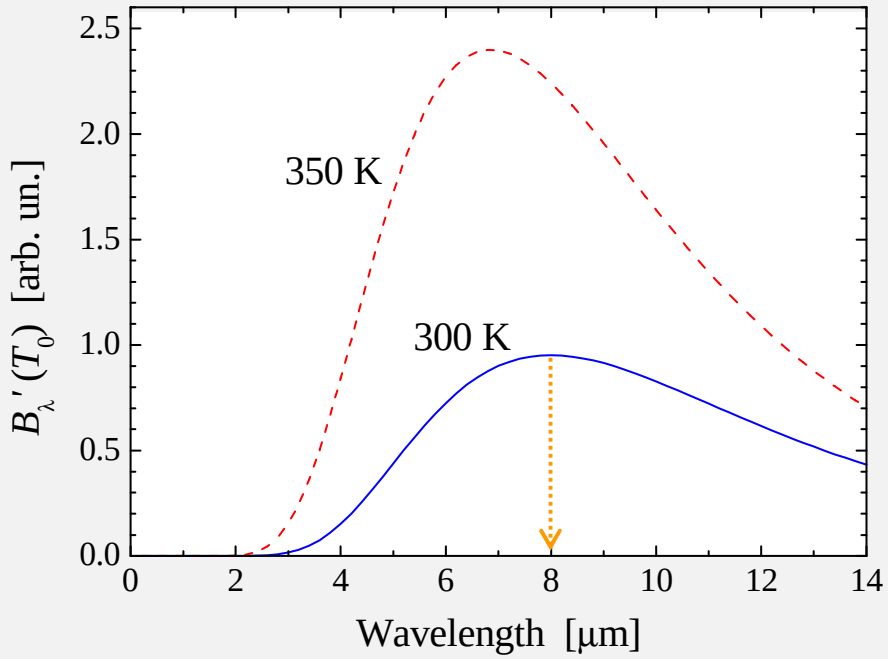

PPTR experimental setup

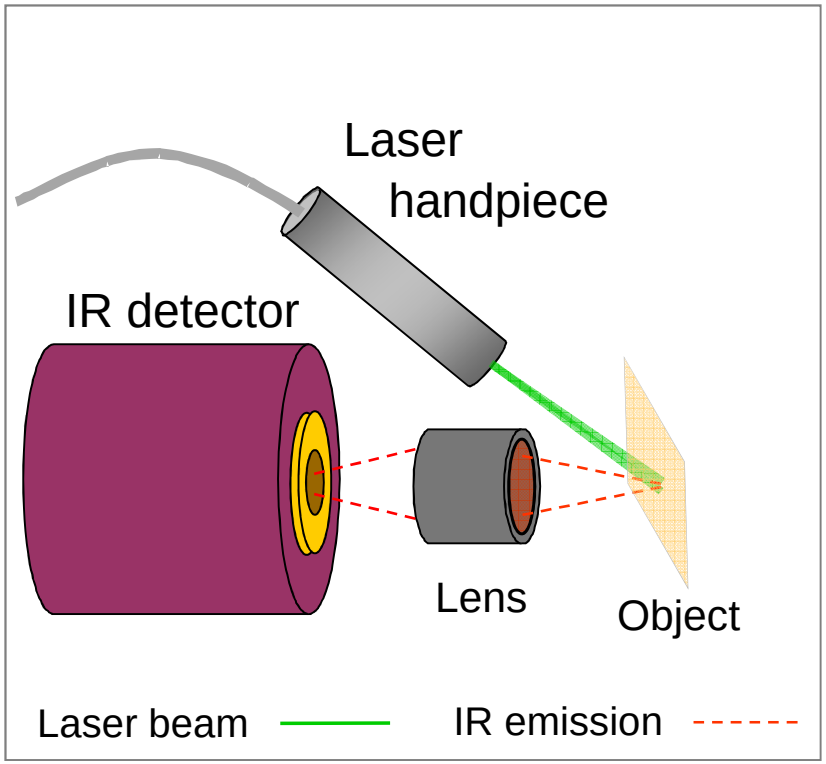

Fast IR camera (FLIR SC7500):

- λ_{acq} = 3.5–5.1 mm
- ν_{acq} = 1000 fps (80 x 100 px)
- $AOI \leq$ 1.5 x 1.5 mm^2

PPTR experimental setup

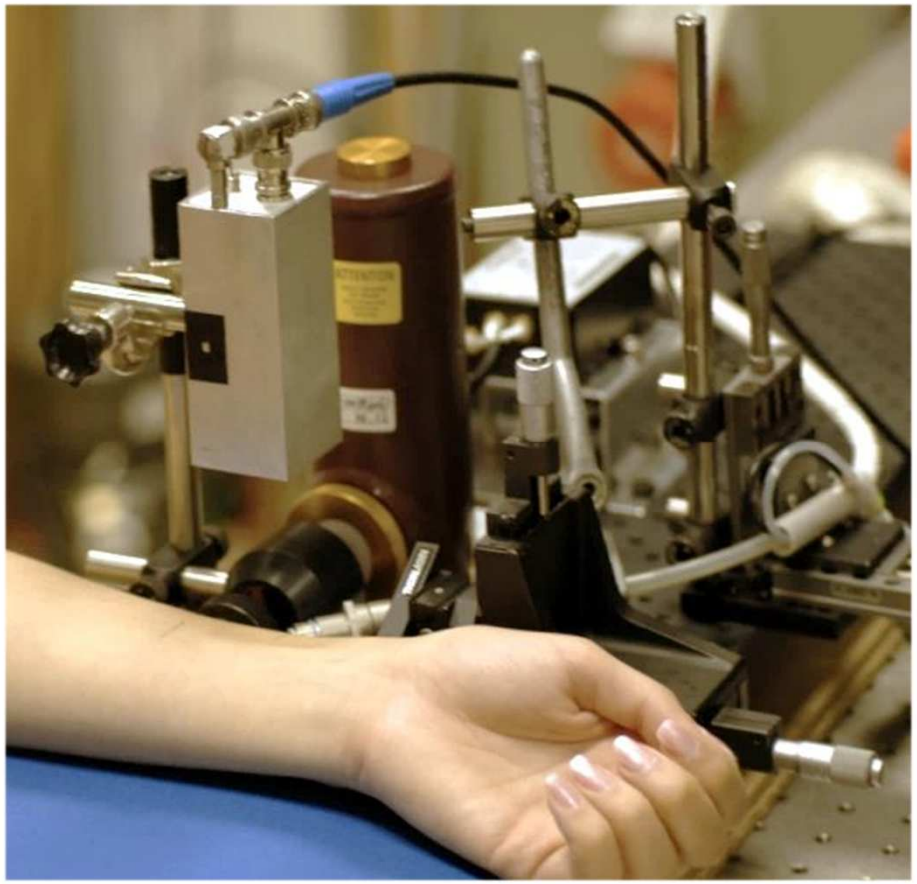

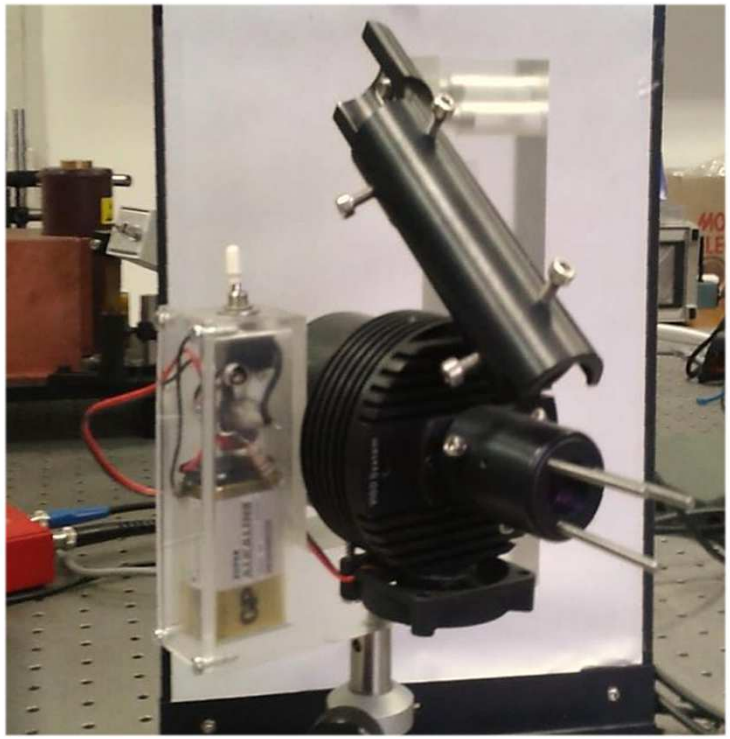

Portable system:

Vigo Systems, PVI-2TE-6

- HgCdZnTe (λ = 3.0–6.2 µm)
- 2-stage TEC cooled (–40 °C)
- $\nu_{acq} \leq$ 20 kHz, AOI: 1 x 1 mm^2

IR detector:

- InSb (λ = 3.0–5.6 µm), LN cooled
- $\nu_{acq} \leq$ 50 kHz, AOI: ϕ = 1 mm

Photodiode (for precise synchronization)

Variation of μ_{IR} within the acquisition spectral band

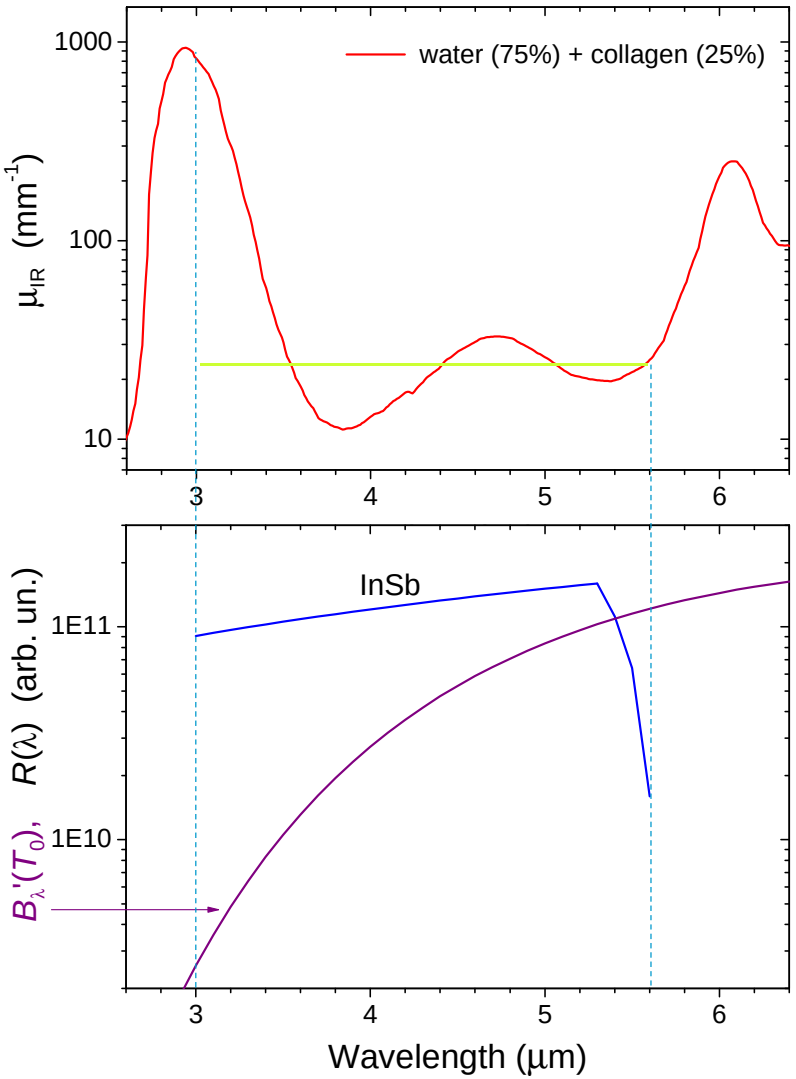

Broad-band IR signal acquisition:

$$\Delta S(t) = C \int_{\lambda_{low}}^{\lambda_{high}} \mu_{IR}(\lambda)\, R(\lambda)\, B_\lambda'(T_b) \int_{z=0}^{\infty} \Delta T(z,t)\, e^{-\mu_{IR}(\lambda) z}\, dz\, d\lambda$$

Monochromatic approximation:

$$\Delta S(t) = C\, \mu_{eff}\, B_\lambda'(T_b) \int_{z=0}^{\infty} \Delta T(z,t)\, e^{-\mu_{eff} z}\, dz$$

- How critical is the selection of μ_{eff} ?
- How to determine the optimal μ_{eff} value ?
- Does use of this approximation limit the performance of PPTR analysis in biological tissues ?

Majaron et al., Phys. Med. Biol. 47, 1929 (2002)

Note: Reconstruction quality depends critically on μ_{eff} !

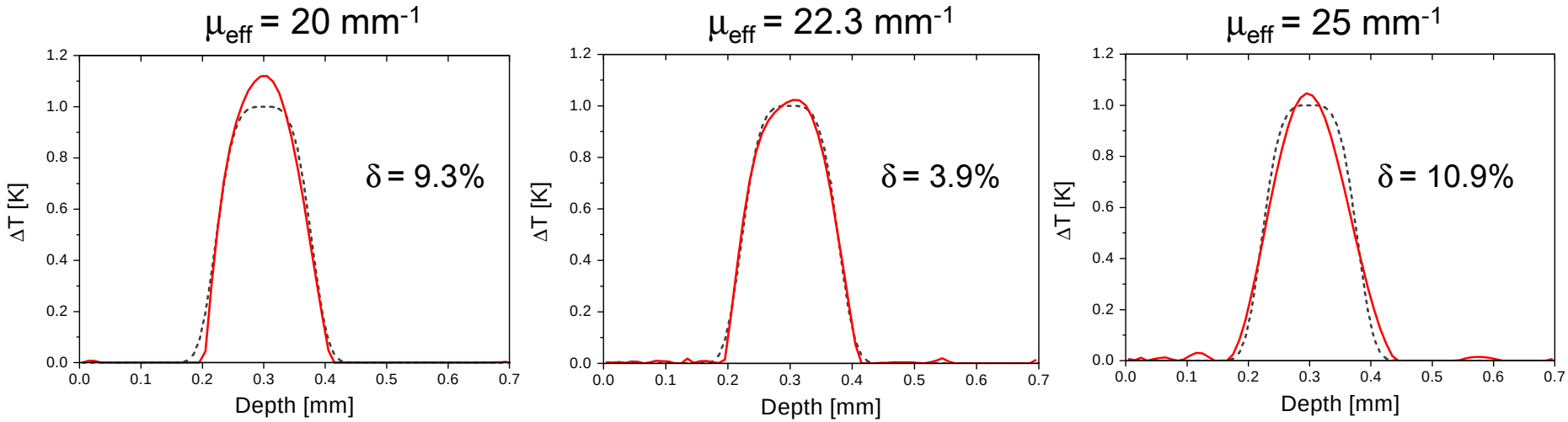

A 10% deviation from the optimal μ_{eff} value introduces significant artifacts !

$$\delta = \frac{\|\text{image} - \text{object}\|}{\|\text{object}\|}$$

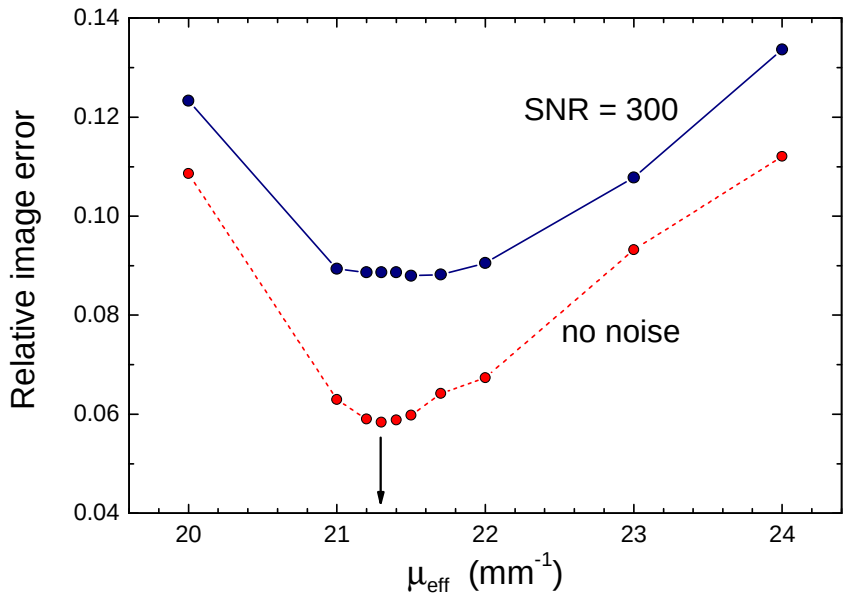

Majaron and Milanič, Phys. Med. Biol. 53, 255 (2008)

Optimal μ_{eff} - our analytical approach

$$\mu_{\mathrm{eff}}\, e^{-\mu_{\mathrm{eff}} z} = \frac{\int_{\lambda_{\mathrm{low}}}^{\lambda_{\mathrm{high}}} R(\lambda)\, B_{\lambda}'(T_0)\, \mu_{\mathrm{IR}}(\lambda)\, e^{-\mu_{\mathrm{IR}}(\lambda) z}\, d\lambda}{\int_{\lambda_{\mathrm{low}}}^{\lambda_{\mathrm{high}}} R(\lambda)\, B_{\lambda}'(T_0)\, d\lambda}$$

Majaron et al., Phys. Med. Biol. 47, 1929 (2002)

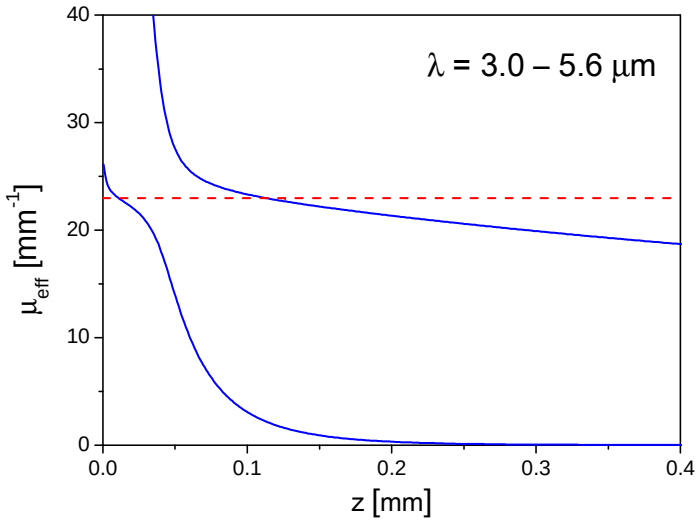

Optimal value of μ_{eff} :

$$\mu_{\mathrm{opt}} = \frac{\sum_i \mu_{\mathrm{eff}}(z_i)\, \exp[-\mu_{\mathrm{eff}}(z_i)\, z_i]}{\sum_i \exp[-\mu_{\mathrm{eff}}(z_i)\, z_i]}$$

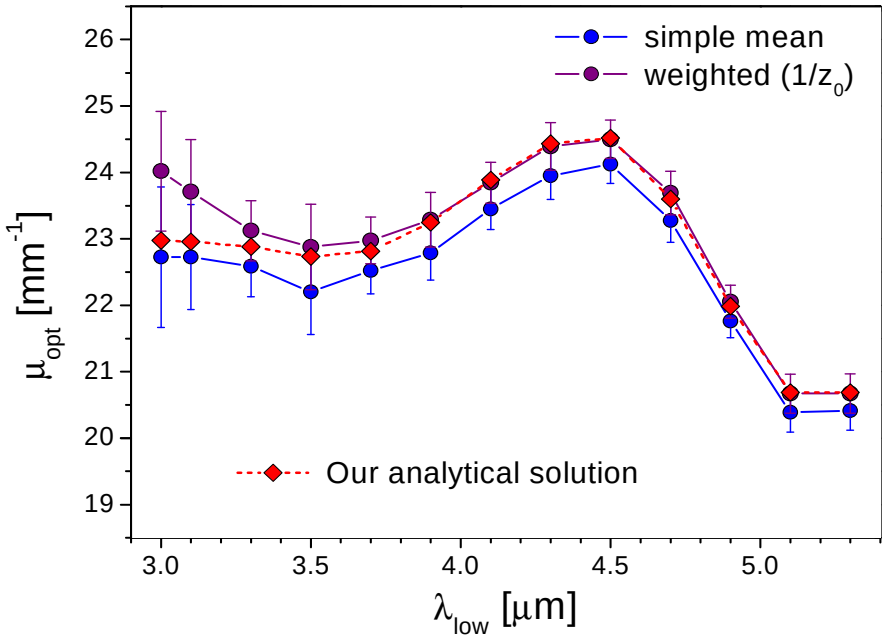

Majaron and Milanič, Phys. Med. Biol. 53, 255 (2008)

Introduction of multispectral kernel function

Layered agar gel sample

- agar powder (2.5 wt.%)
- distilled water
- TiO_2 powder (for scattering)

Absorbing layer:

- colored polyethilene foil (d ~ 7 μm)
- at different depths (z = 40–900 μm)

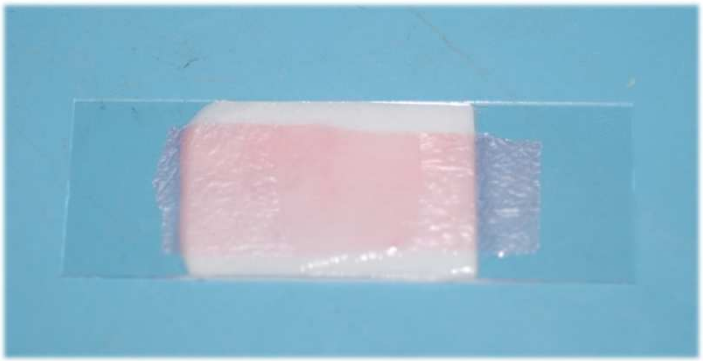

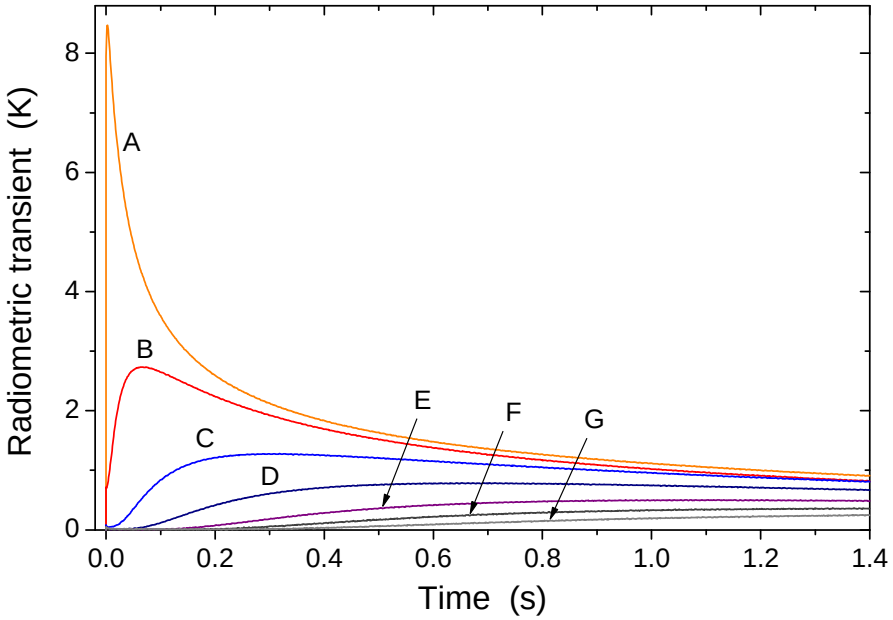

Custom reconstruction code:

- multispectral kernel function *
- minimization using the ν-method *
- non-uniform signal binning **
- non-negativity constraint

** Milanič et al, Phys. Med. Biol. 54, 2829 (2009)*

*** Milanič et al., Proc. SPIE, 7731-0O (2009)*

Evaluation of PPTR temperature profiling *in vitro*

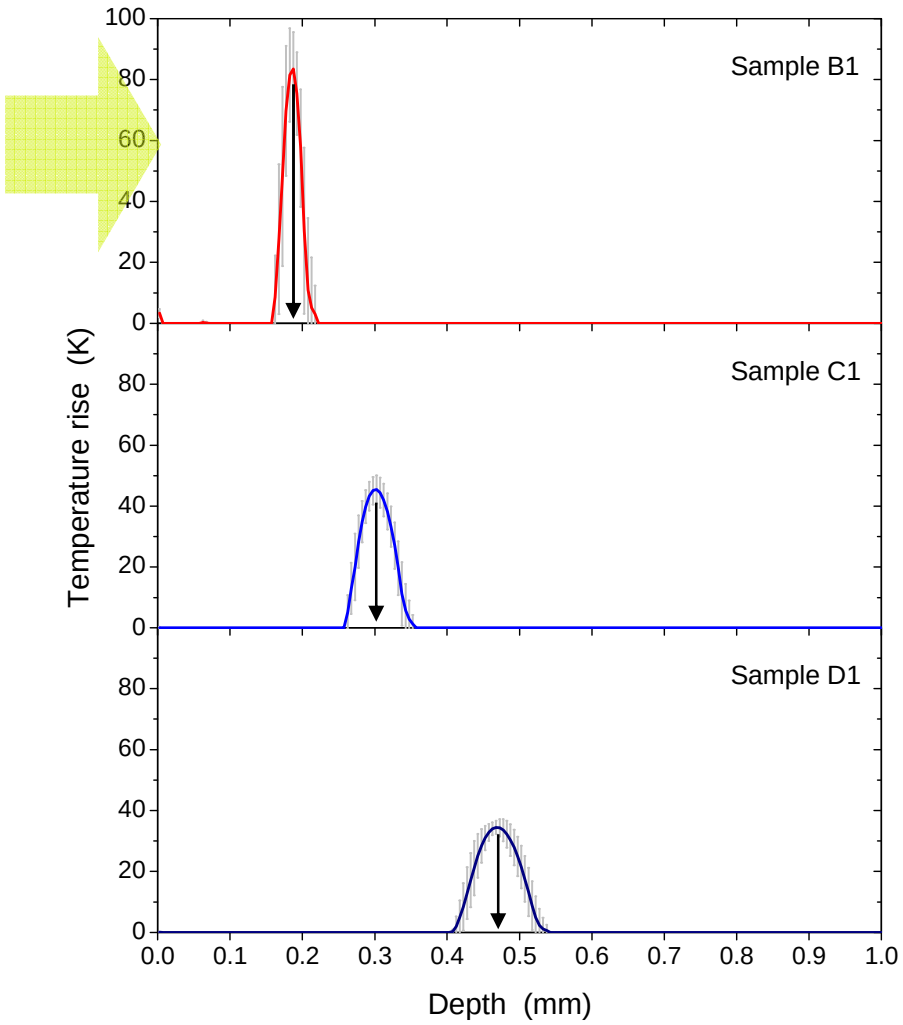

μMRI image (3D spin echo, T_1-weighted)

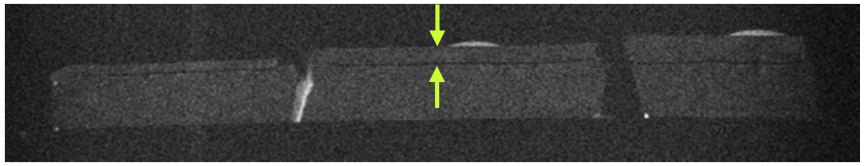

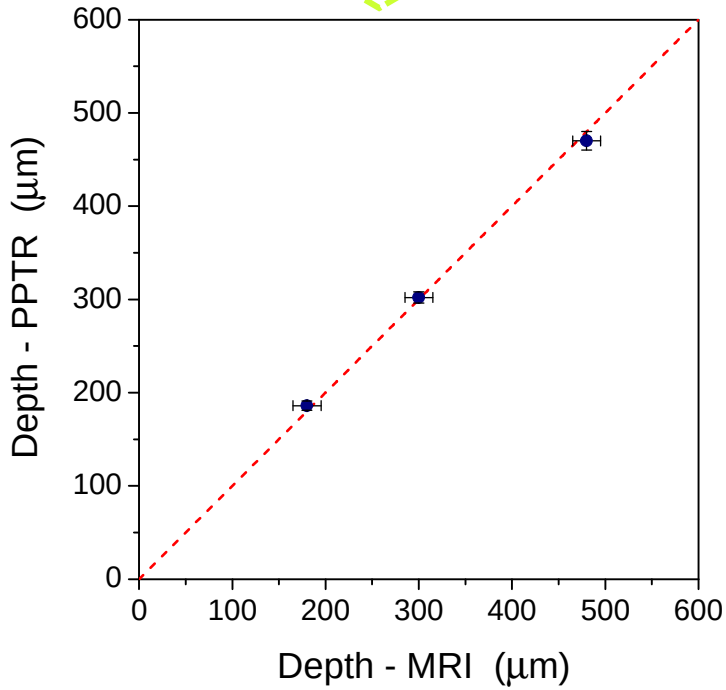

PPTR-determined absorber depths match the results from high-resolution MRI.

Milanič et al, Phys. Med. Biol. 54, 2829 (2009)

Evaluation of PPTR temperature profiling *in vitro*

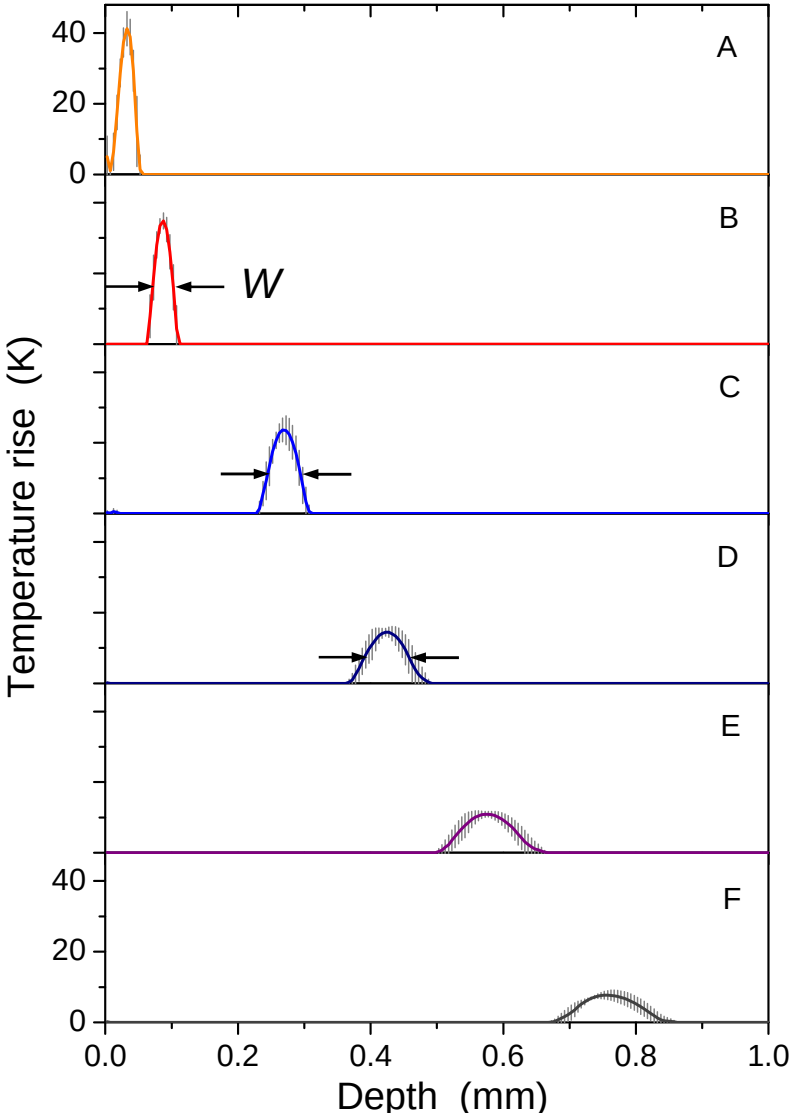

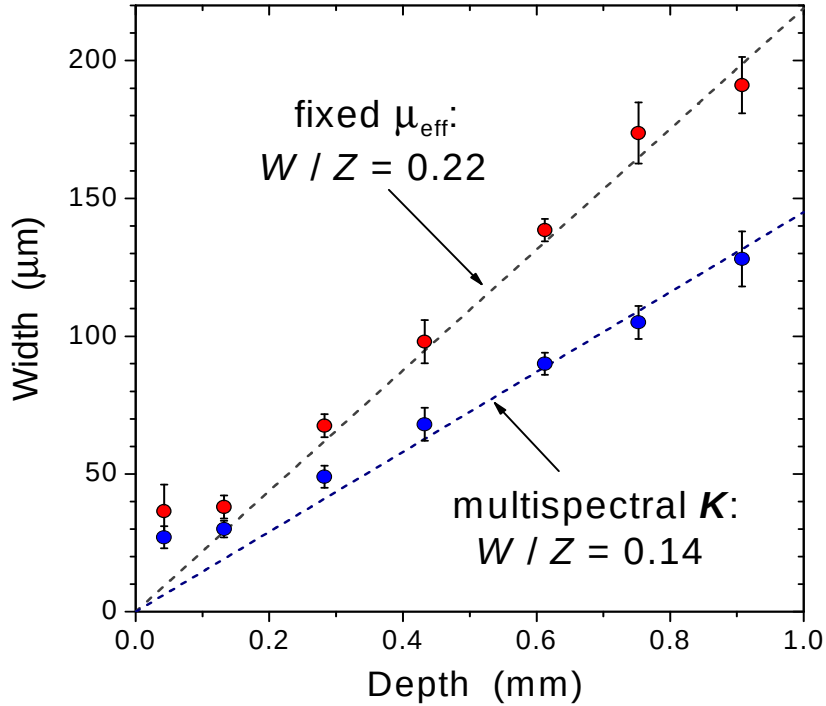

Introduction of the spectrally composite kernel matrix ***K*** significantly reduces the broadening artefact.

- earlier record: $W \sim 0.5\,Z$ (in simulation)

Milanič et al, Phys. Med. Biol. 54, 2829 (2009)

Majaron & Milanič, J. Phys: Conf. Ser. 214, 012007 (2010)

Summary 1 - PPTR temperature profiling

Advances in

- forward model formulation (= spectrally composite kernel),
- signal preconditioning (nonuniform binning), and
- reconstruction algorithms

have enabled temperature depth profiling in biological tissue (phantoms) with signifficantly smaller axial blurring than previously believed possible.

These improvements enable

- development of novel biomedical applications (research, clinical)
- improvements in other PTR applications (material characterization, NDE)

2. In vivo application examples:

Temperature depth profiling

- monitoring of laser tatoo removal
- structural characterization of vascular lesions
- response of a port-wine stain lesion to laser treatment
- Nd:YAP laser (1342 nm) energy deposition in skin
- assessment of the maximal safe radiant exposure

Characterization of tattoos in human skin

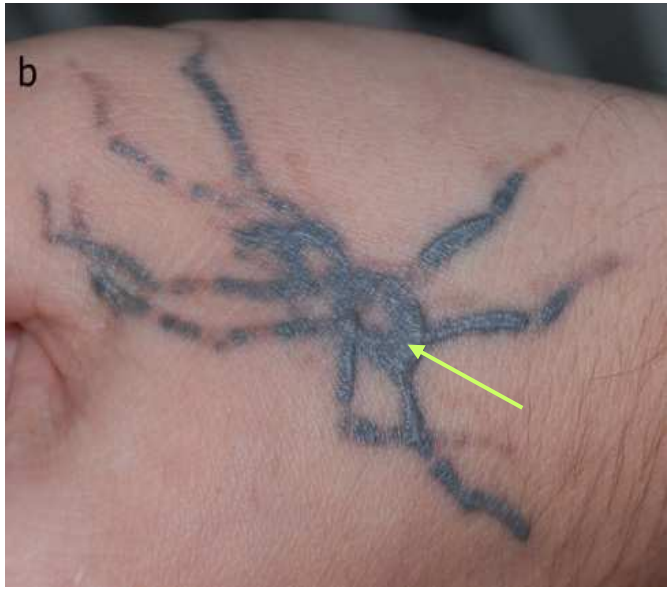

PPTR laser irradiation:

- λ = 1064 nm
- t_p = 5 ms
- H_0 = 7 J/cm^2

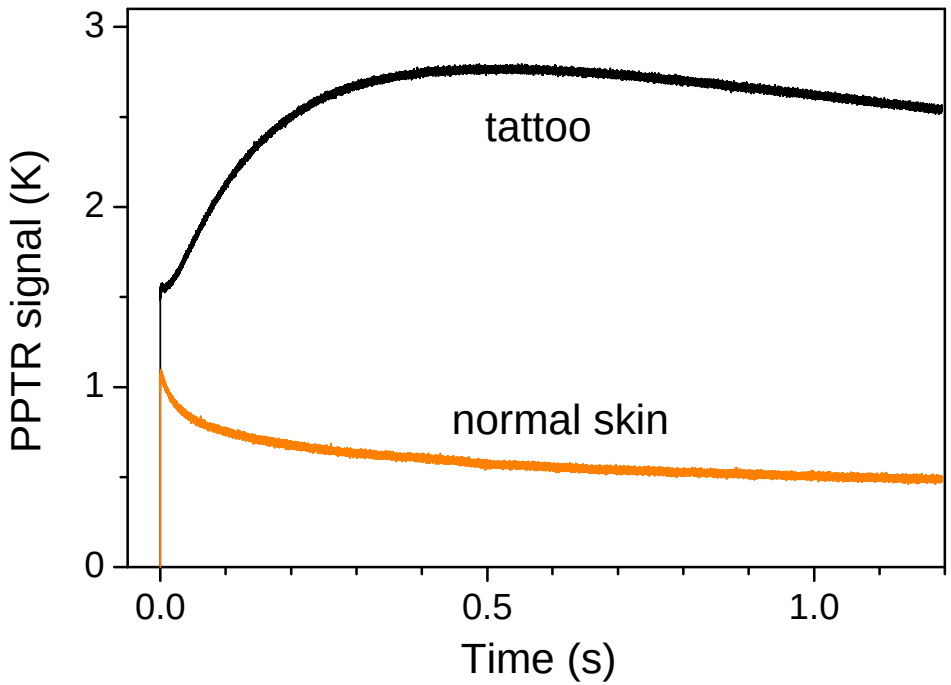

IR detector:

- InSb, LN cooled
- λ_{acq} = 3.0–5.6 µm
- ν_{acq} = 50,000 Hz
- FOV = ϕ 1 mm

Milanič & Majaron, Proc. SPIE, 8207-0G (2012); J. Laser Health Acad., 68 (2013)

Monitoring of laser tattoo removal

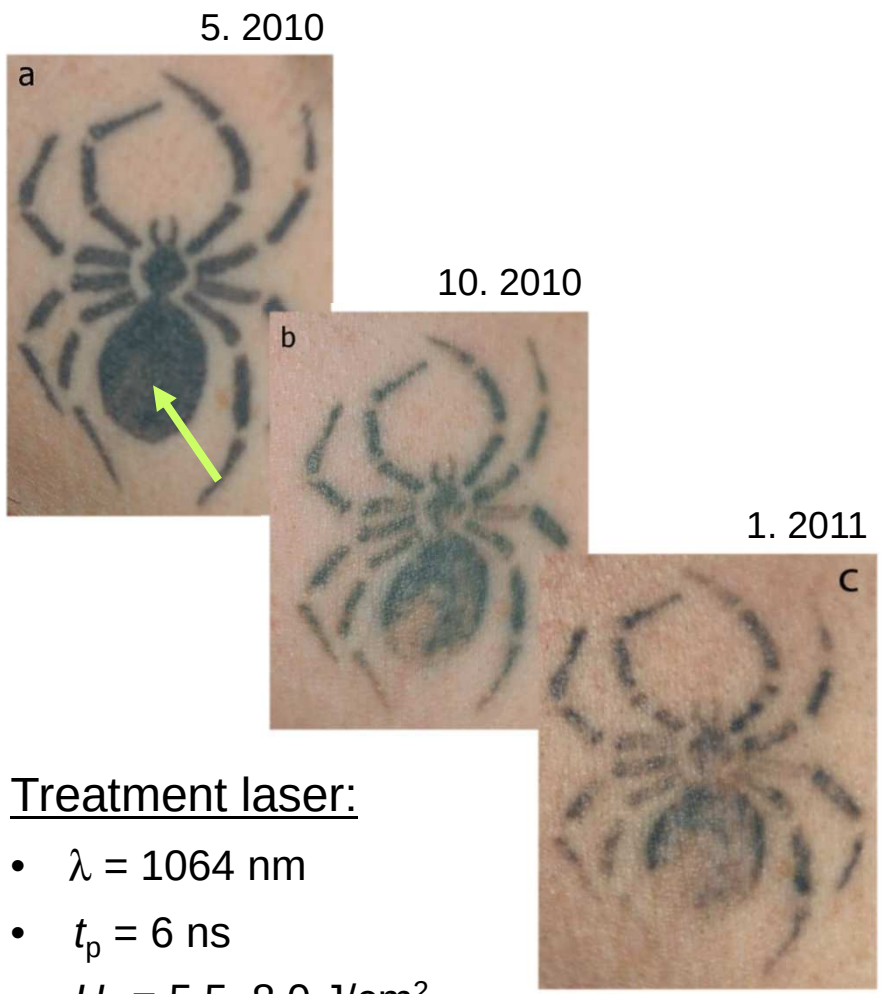

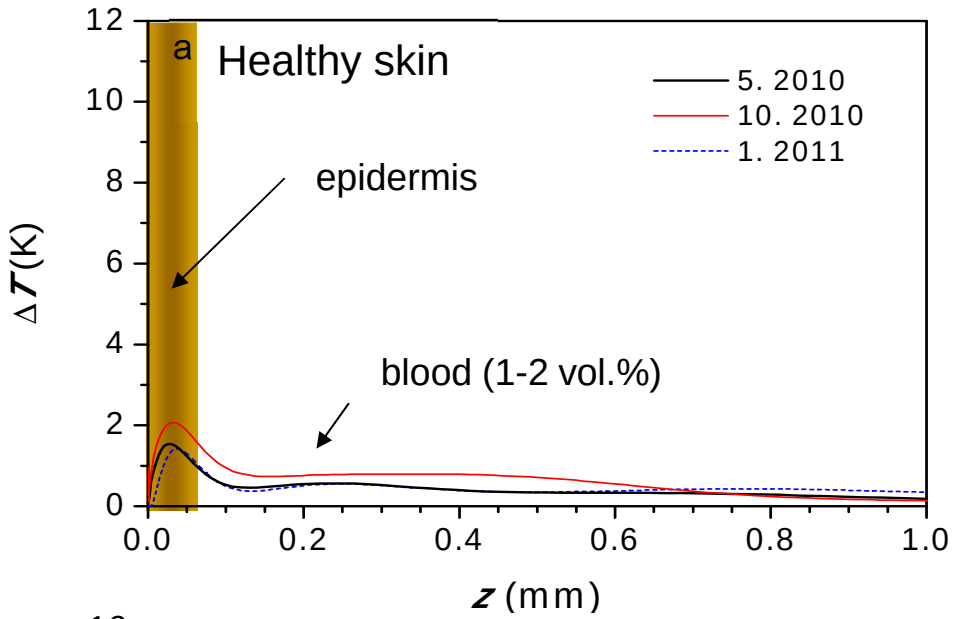

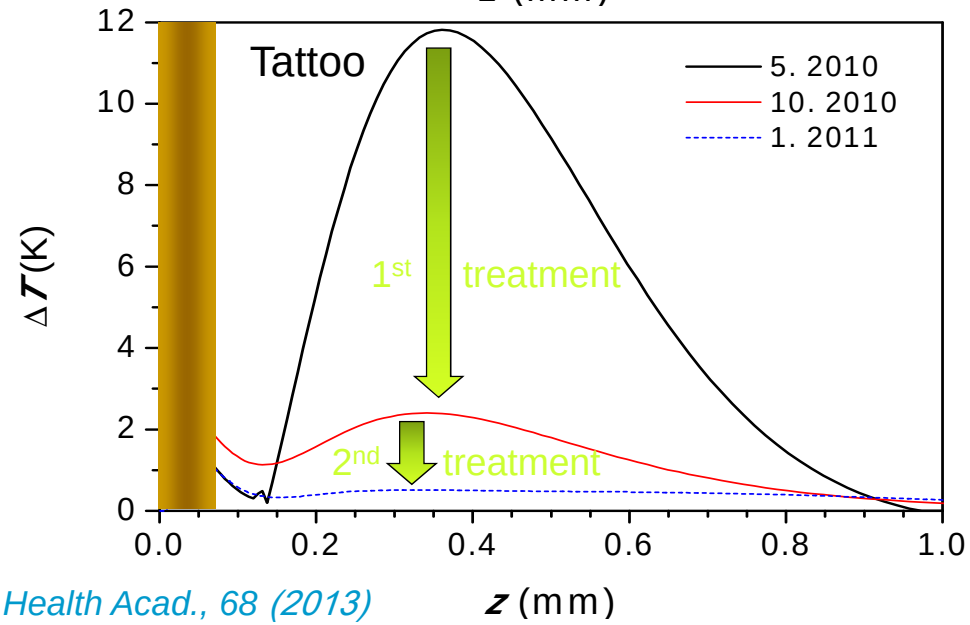

Treatment laser:

- λ = 1064 nm
- t_p = 6 ns
- H_0 = 5.5–8.0 J/cm^2

(QX Max, Fotona, Slovenia)

Milanič & Majaron, Proc. SPIE, 8207-0G (2012); J. Laser Health Acad., 68 (2013)

Monitoring of laser tattoo removal

before treatment

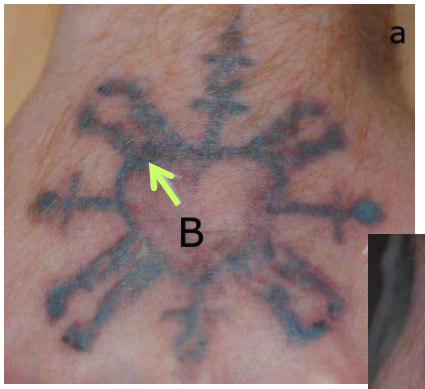

after
1st treatment

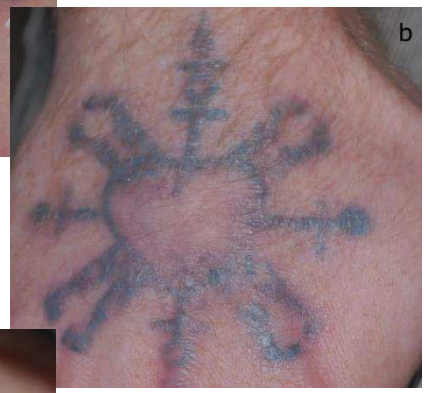

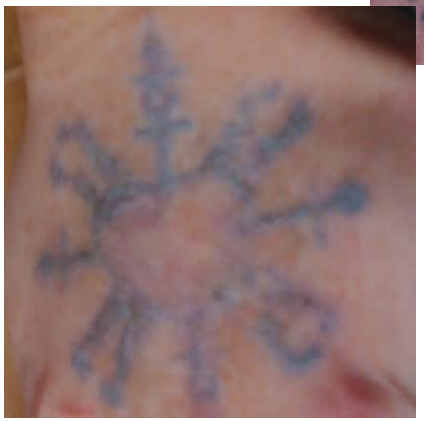

after
2nd treatment

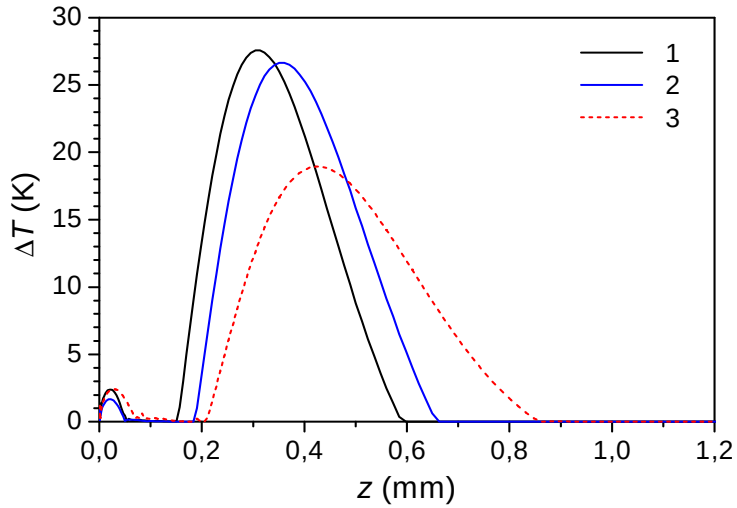

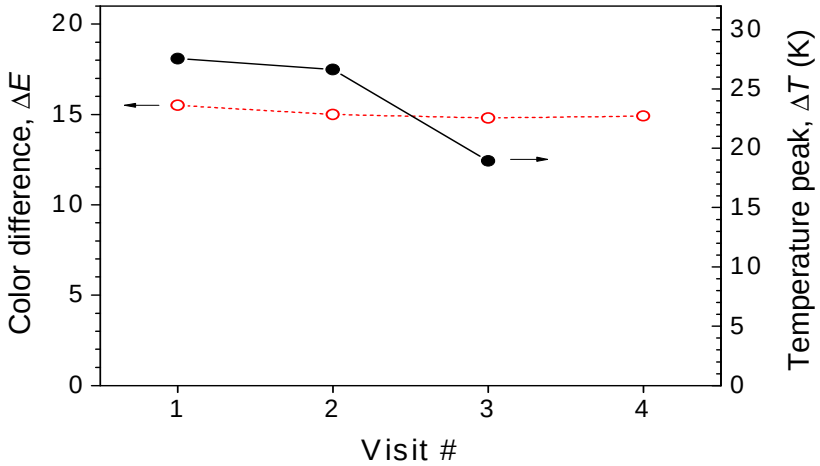

PPTR profiling reveals that the tattoo pigment undergoes gradual degradation and removal, although visual impression is not (yet) affected.

Milanič & Majaron, Proc. SPIE, 8207-0G (2012); J. Laser Health Acad., 68 (2013)

Anatomy of human skin and port-wine stain (PWS)

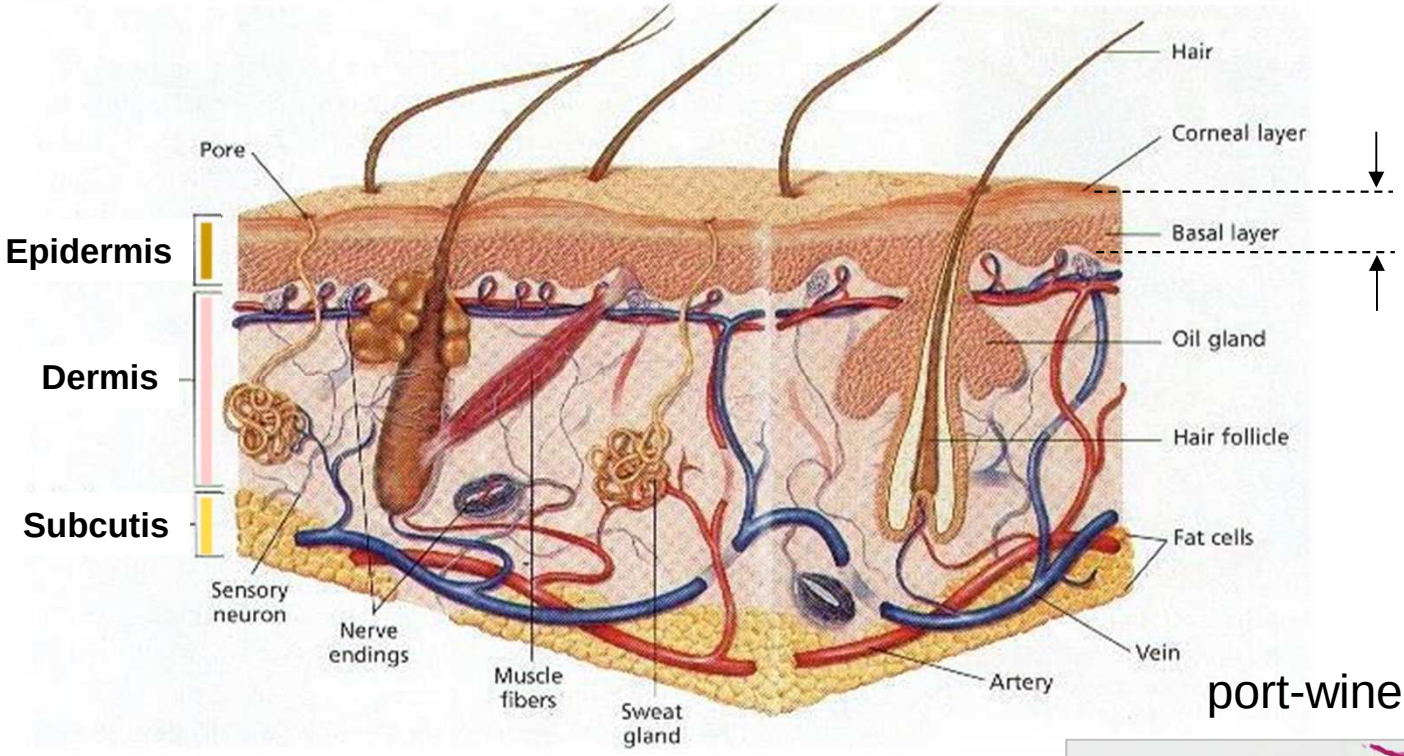

50-150 µm

Histology of a port-wine stain (PWS) lesion

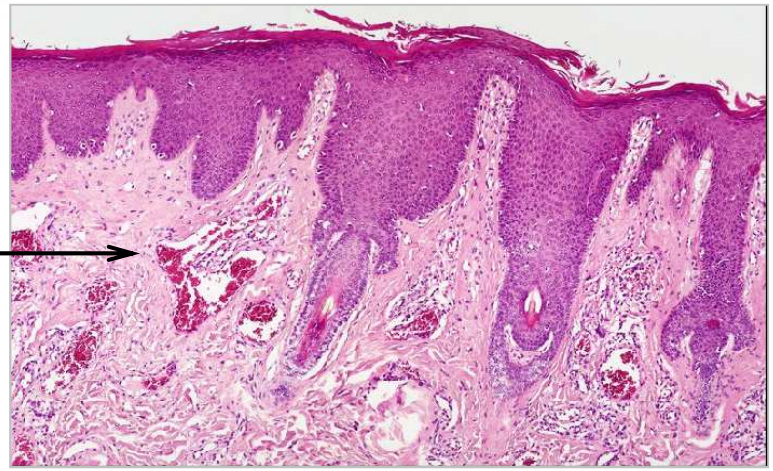

enlarged blood vessels in the upper dermis

- 20–100 µm in diameter
  - up to 10 vol.%

Depth of microvasculature in a port-wine stain

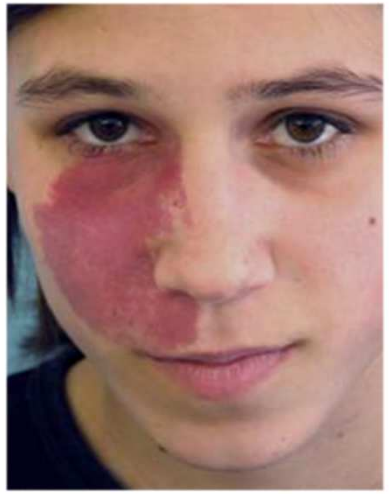

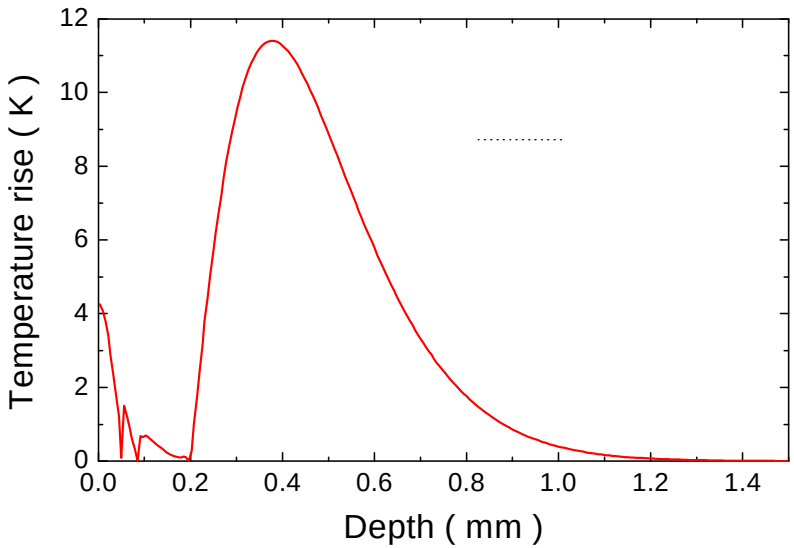

Temperature depth profile from PPTR

(585 nm, 1.5 ms)

Comparison with Optical Doppler Tomography :

OCT :
Amplitude image (scatter)

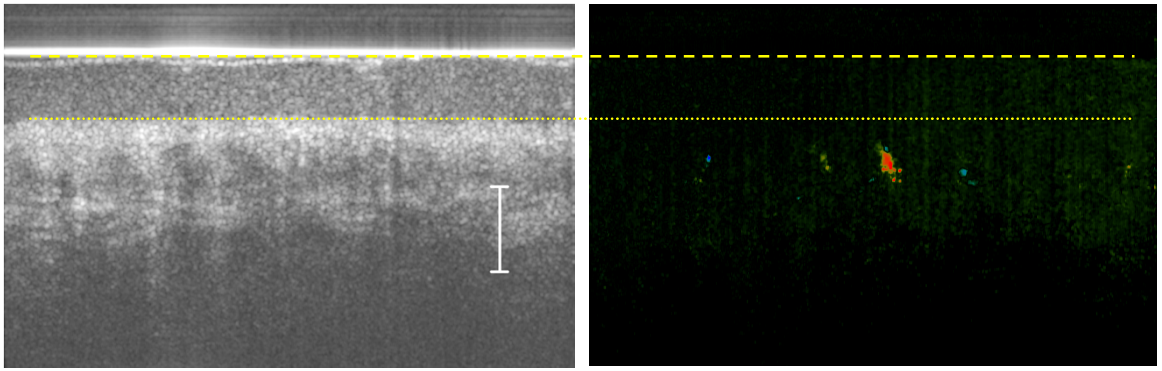

ODT :
Doppler image (velocity)

z_{PWS} ~ 220 µm (n = 1.40)

Li et al., J. Biomed. Opt. 9, 961 (2004)

Study of PWS response to laser treatment

PWS patient:

- female
- fair skin
- laser-treated before

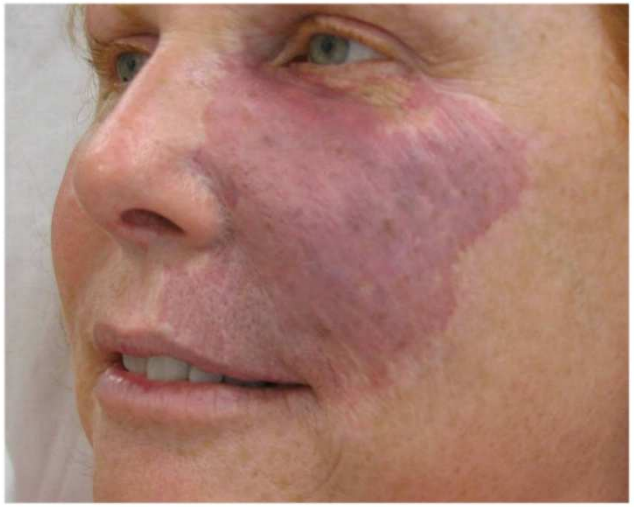

Hypothesis:

- 532 nm heating produces met-hemoglobin
- increases blood absorption at 1064 nm

Vascular laser:

- λ = 532 nm + 1064 nm
- t_p = 25 ms
- H_0 incrementally increased

Majaron et al., Laser Surg. Med. sup. 21, 49 (2009)

Study of PWS response to laser treatment

Radiant exposure incrementally increased: H_0 = 1.8 – 9.0 J/cm^2

- pulse structure: 4 x 1 ms; sequence duration: t_p = 25 ms

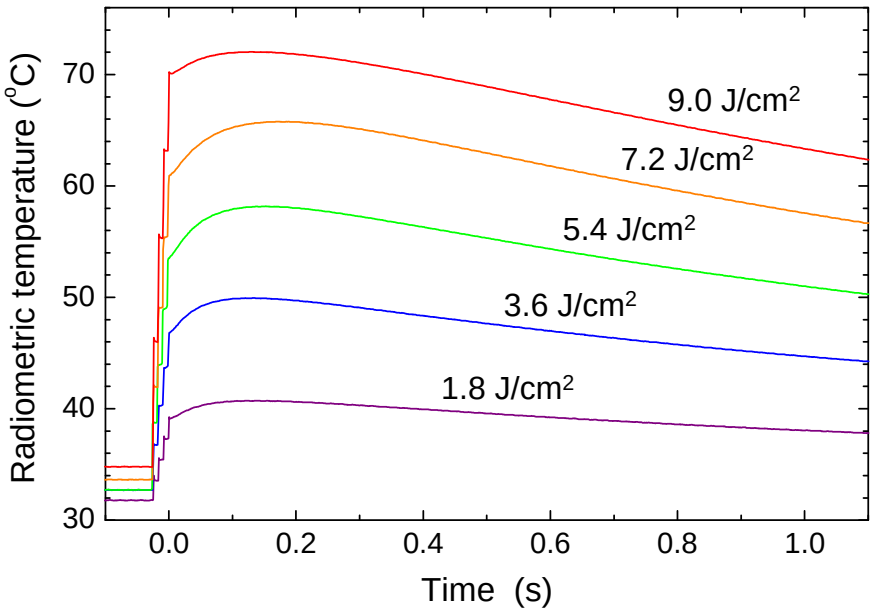

after

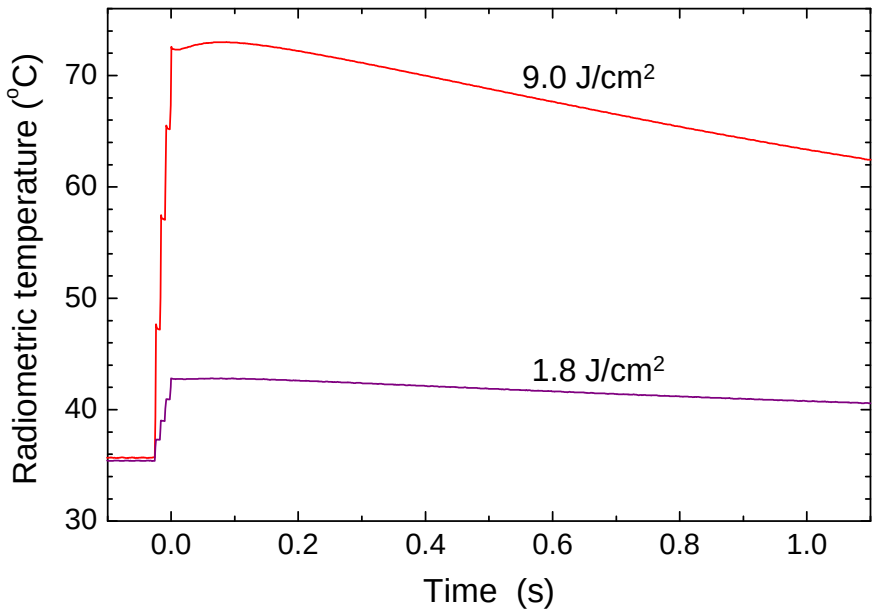

After the pulse sequence (8 pulses, 34 J/cm^2), PPTR signals are different

Majaron et al., Laser Surg. Med. sup. 21, 49 (2009)

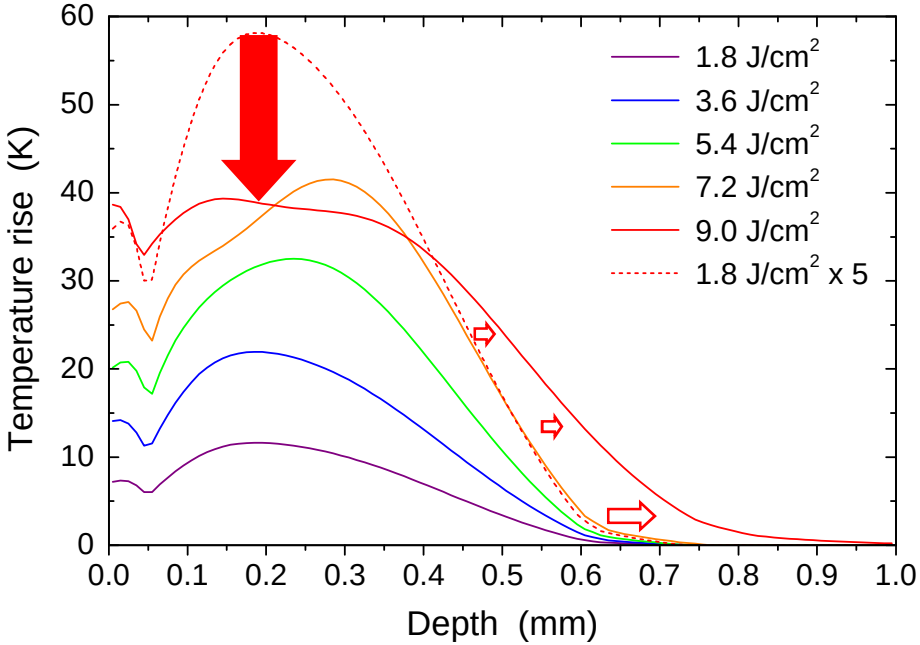

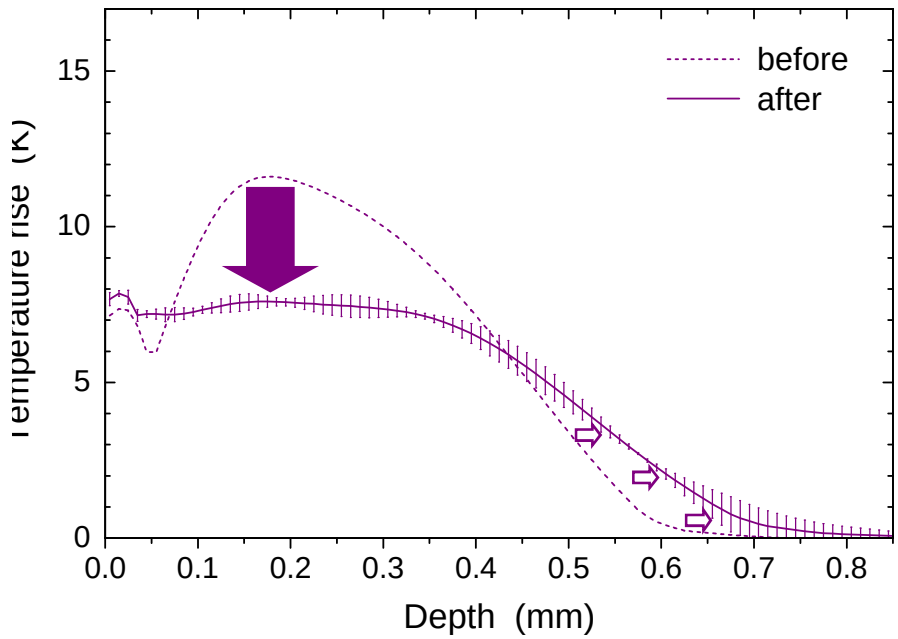

Absorption in the superficial PWS layer is irreversibly reduced
at radiant exposures above 5-6 J/cm^2

→ laser energy reaches deeper into the dermis (PWS)

→ epidermal heating is enhanced (more backscatter, higher fluence)

Results are consistent with conversion of HbO to metHb

- drop in 532 nm absorption (23 → 15 mm^{-1})
- The observed threshold matches earlier reported values (65–72.5 °C; 5 J/cm^2)

Majaron et al., Laser Surg. Med. sup. 21, 49 (2009)

Same experiment repeated on healthy skin

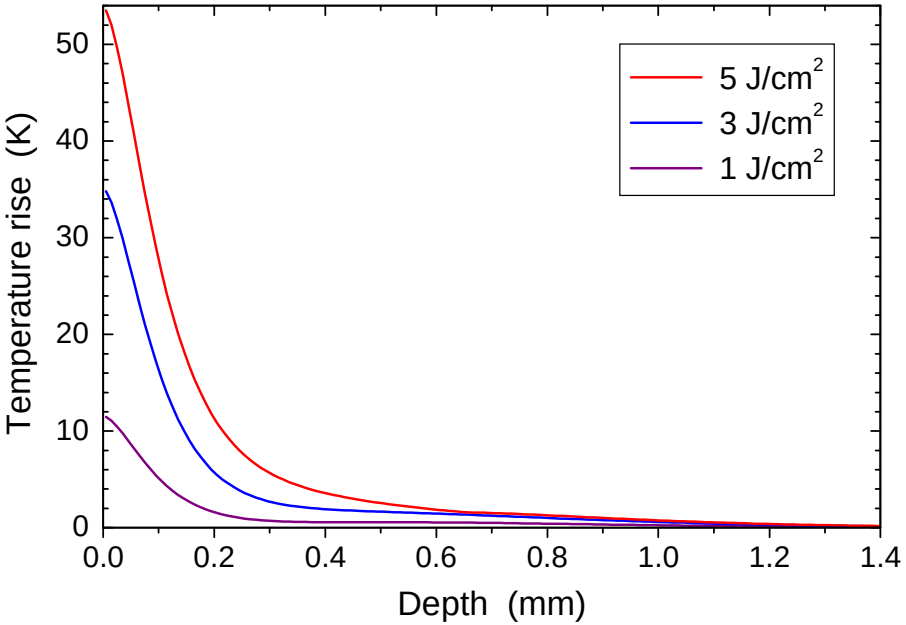

after

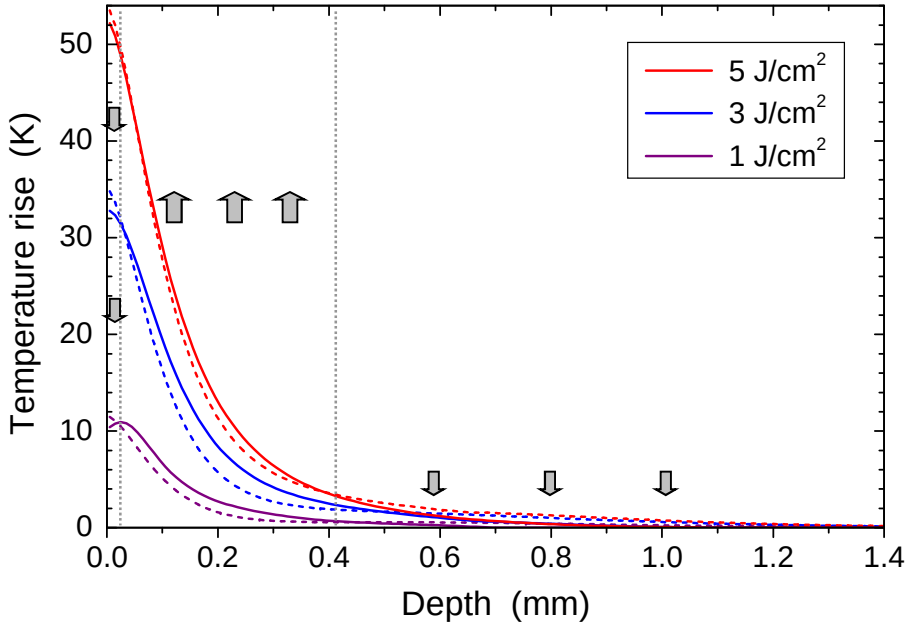

Enhanced energy deposition in the upper dermis (z < 0.4 mm)

→ reduced penetration depth

→ reduced epidermal fluence (less backscatter)

Results are consistent with persistent erythema

Majaron et al., Laser Surg. Med. sup. 21, 49 (2009)

Energy deposition profile of a 1342 nm Nd:YAP laser in human skin

PPTR signals from healthy skin sites:

- shoulder (outer), forearm (inner)
- detection area: 1.5 x 1.5 mm^2

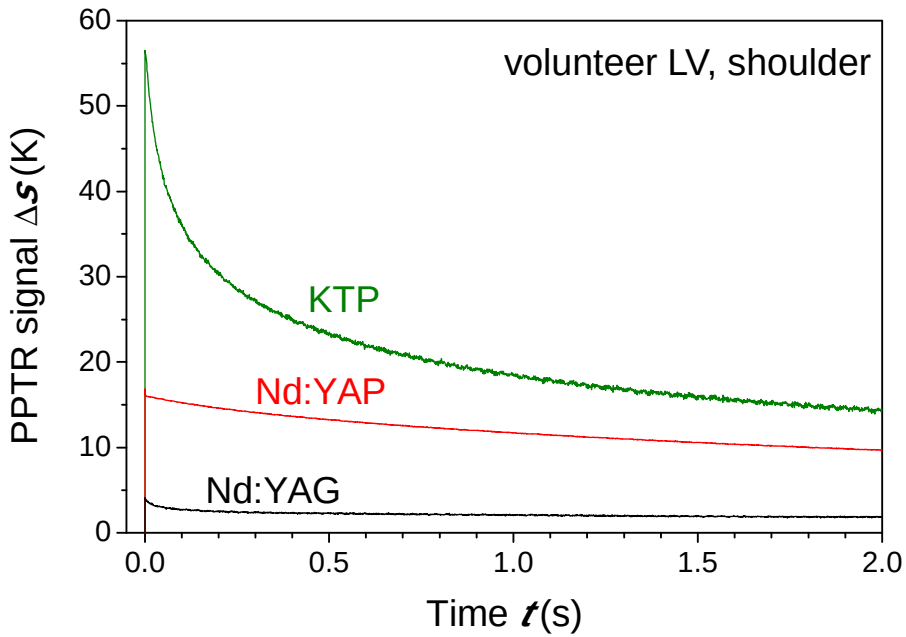

(Signals are normalized to H_0 = 10 J/cm^2)

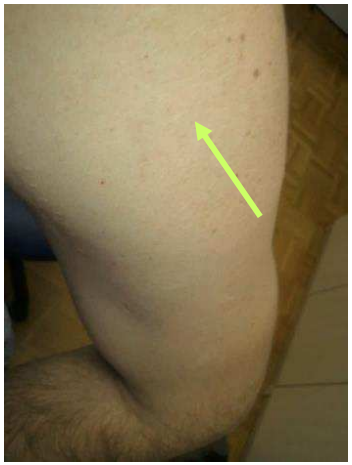

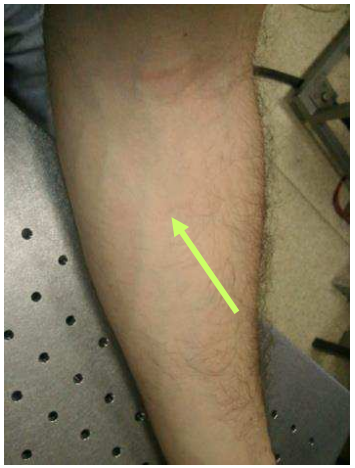

Custom reconstruction code:

- non-uniform signal binning
- multispectral kernel
- minimization using the ν-method
- non-negativity constraint

Milanič and Majaron, Laser Surg. Med. 45, 8 (2013)

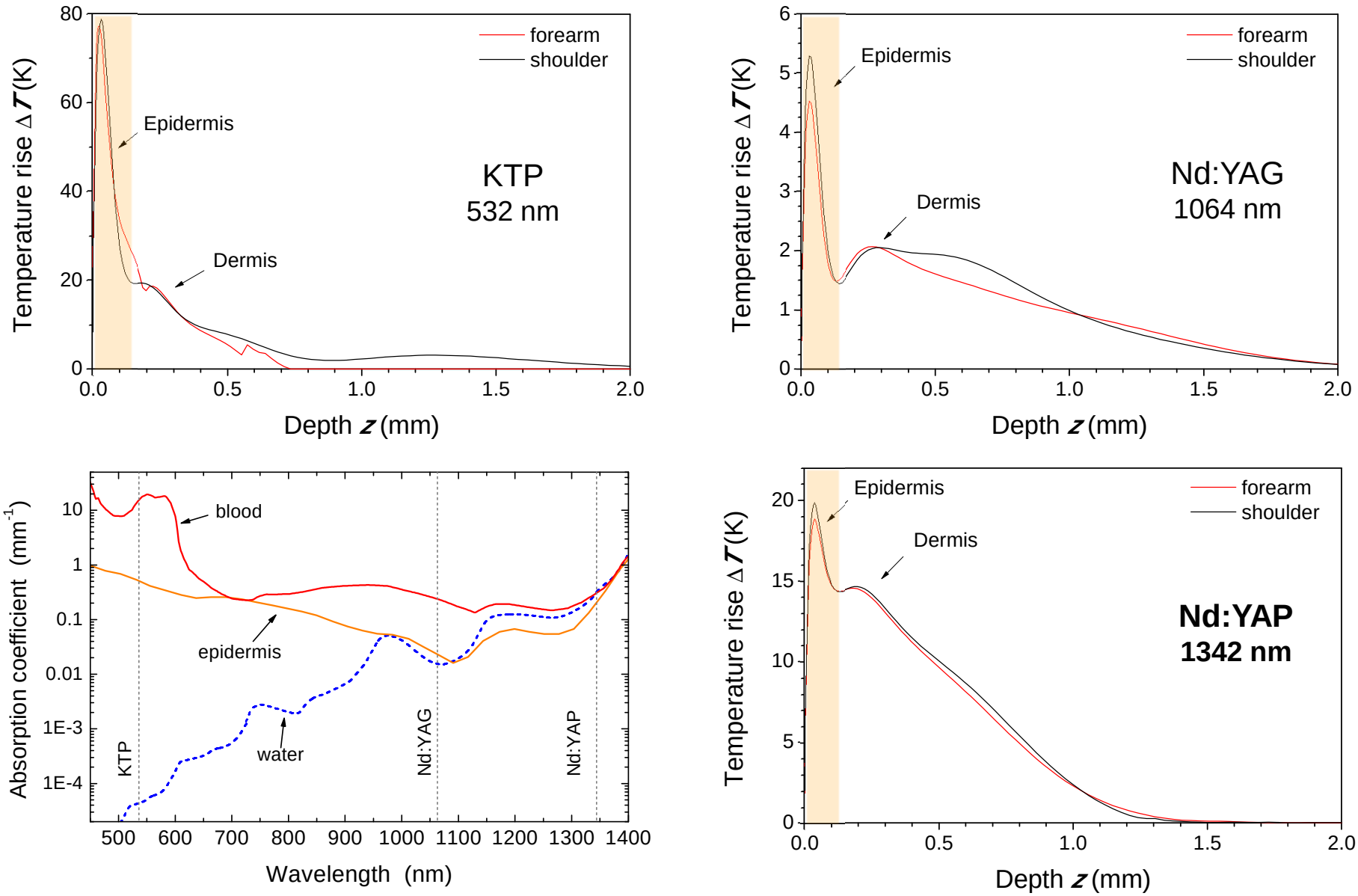

(All profiles normalized to H_0 = 10 J/cm^2)

Milanič and Majaron, Laser Surg. Med. 45, 8 (2013)

Energy deposition in normal skin at 1342 nm vs. 1064 nm

Temperature profiles induced in the same site with two lasers, scaled to reach the same epidermal temperature rise:

(volunteer LV, shoulder)

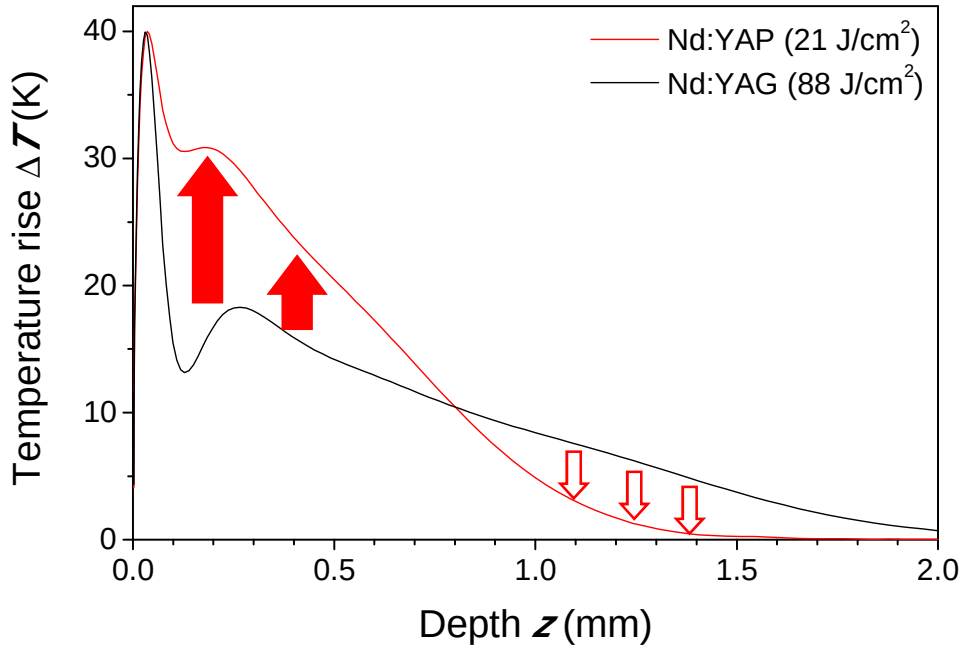

Nd:YAP laser is very suitable for controlled heating of the upper dermis, as required for non-ablative skin rejuvenation.

Risks of overheating the epidermis and subcutis are significantly reduced compared to the Nd:YAG laser.

Quantitative comparison with the familiar Nd:YAG laser enables design of a safe and effective clinical protocol.

Milanič and Majaron, Laser Surg. Med. 45, 8 (2013)

Prediction of the maximal safe laser radiant exposure
on individual patient basis

12 healthy volunteers
- males and females
- skin phototypes I–IV

326 distinct test spots
- on the extremities

Alexandrite laser irradiation
- λ = 755 nm, t_p = 3 ms
- d = 8 mm, 12 mm
- H_0 = 10 - 90 J/cm^2
- CS cooling: 30 / 50 ms

The severity of adverse effects:
- crusting and erythema
- 24 hours post treatment
- scored blindly
- on a scale of 1–10

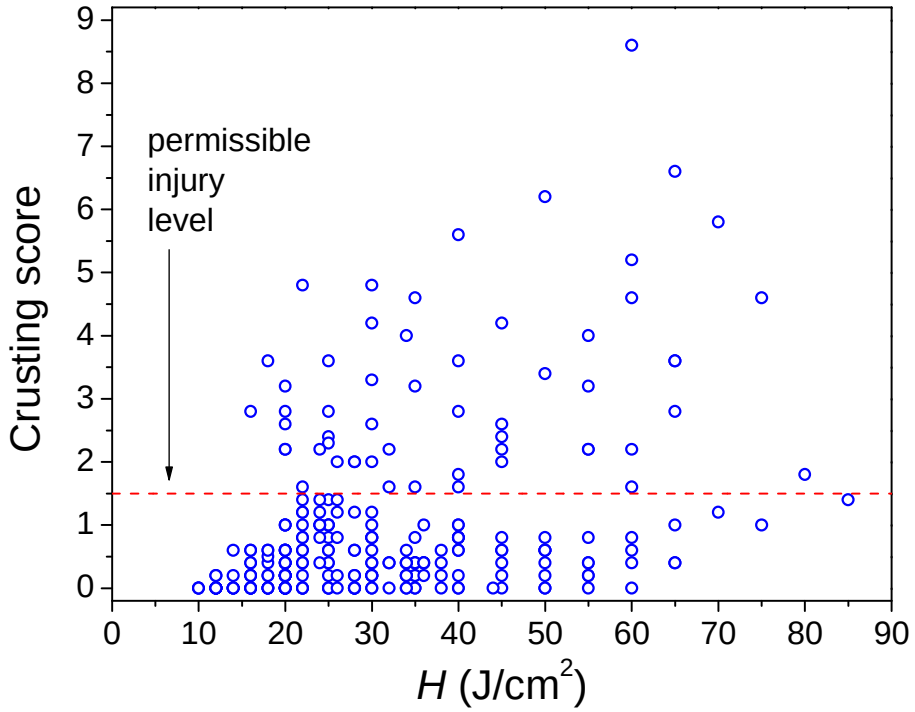

Verkruysse et al., Laser Surg. Med. 39, 757 (2007)

Radiometric measurements at the same test sites

12 healthy volunteers
- males and females
- skin phototypes I–IV

326 distinct test spots
- on the extremities

Alexandrite laser
- λ = 755 nm, t_p = 3 ms
- d = 18 mm
- H_0 = 6 J/cm^2
- no CS cooling

Fast mid-IR camera:
- model „c“ (FLIR, Boston, MA)
- λ_{acq} = 3.0–5.5 µm
- ν_{acq} = 1000 fps
- AOI < 3.5 x 3.5 mm^2

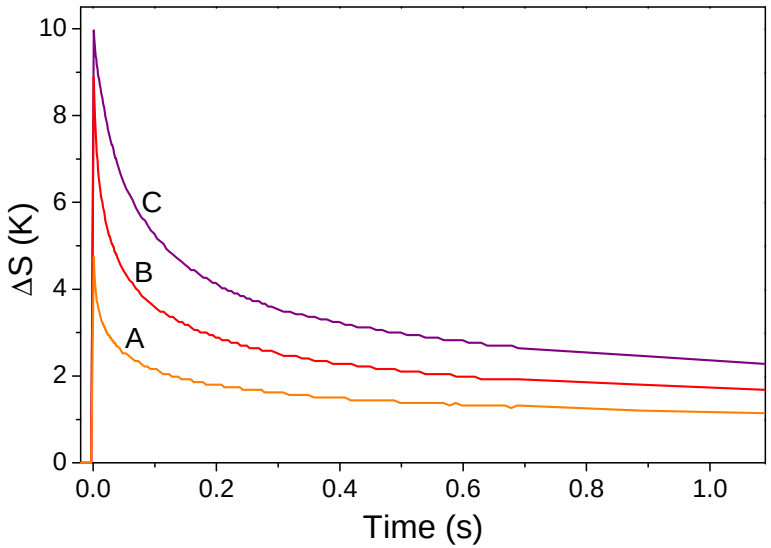

Verkruysse et al., Laser Surg. Med. 39, 757 (2007)

Prediction of the maximal safe radiant exposure

1. For each test site, the laser-induced temperature profile is reconstructed from the recorded PPTR signal, using a custom iterative algorithm.

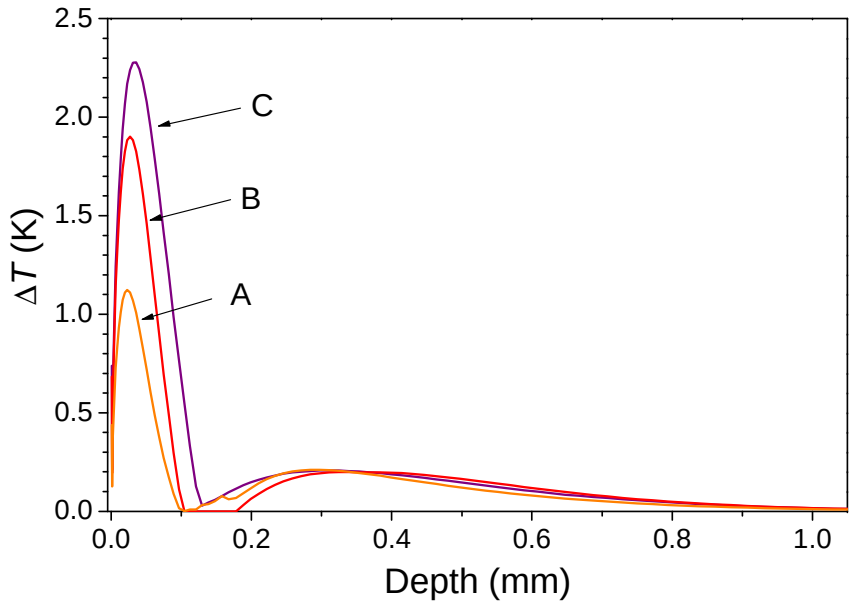

2. From this temperature profile (= initial condition), temperature field evolution and epidermal thermal damage at the clinically applied radiant exposure *H* are predicted using a custom numerical model.

Heat diffusion: $$\rho c_p \frac{\mathrm{d}T(x,z,t)}{\mathrm{d}t} = k \nabla^2 T(x,z,t)$$

Thermal denaturation: $$\Omega(x,z,t) = A \int_0^{\tau} \exp\left(-E_a / RT(x,z,t')\right) \mathrm{d}t'$$

Milanič et al., Lasers Surg. Med. 43, 164 (2011)

Prediction of the maximal safe radiant exposure

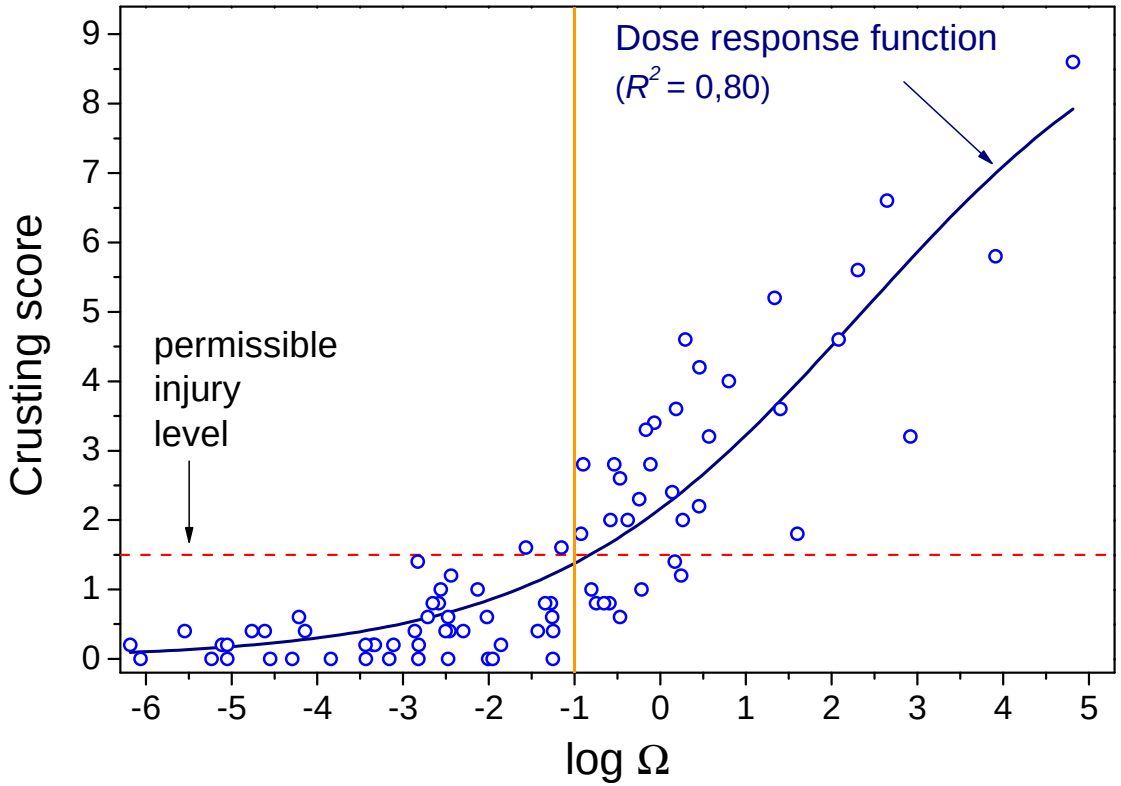

d = 8mm
||S - KT|| < 0.2

Epidermal damage threshold value:

log Ω = -1

3. The same numerical model can now be used to predict the maximal safe laser radiant exposure (H_{max}) for any test site, from its PPTR record.

   This is obtained by gradually increasing the radiant exposure in the numerical model, until the epidermal damage threshold is reached (e.g., log Ω = -1).

Majaron et al., Lasers Surg. Med. sup. 23, 916 (2011)

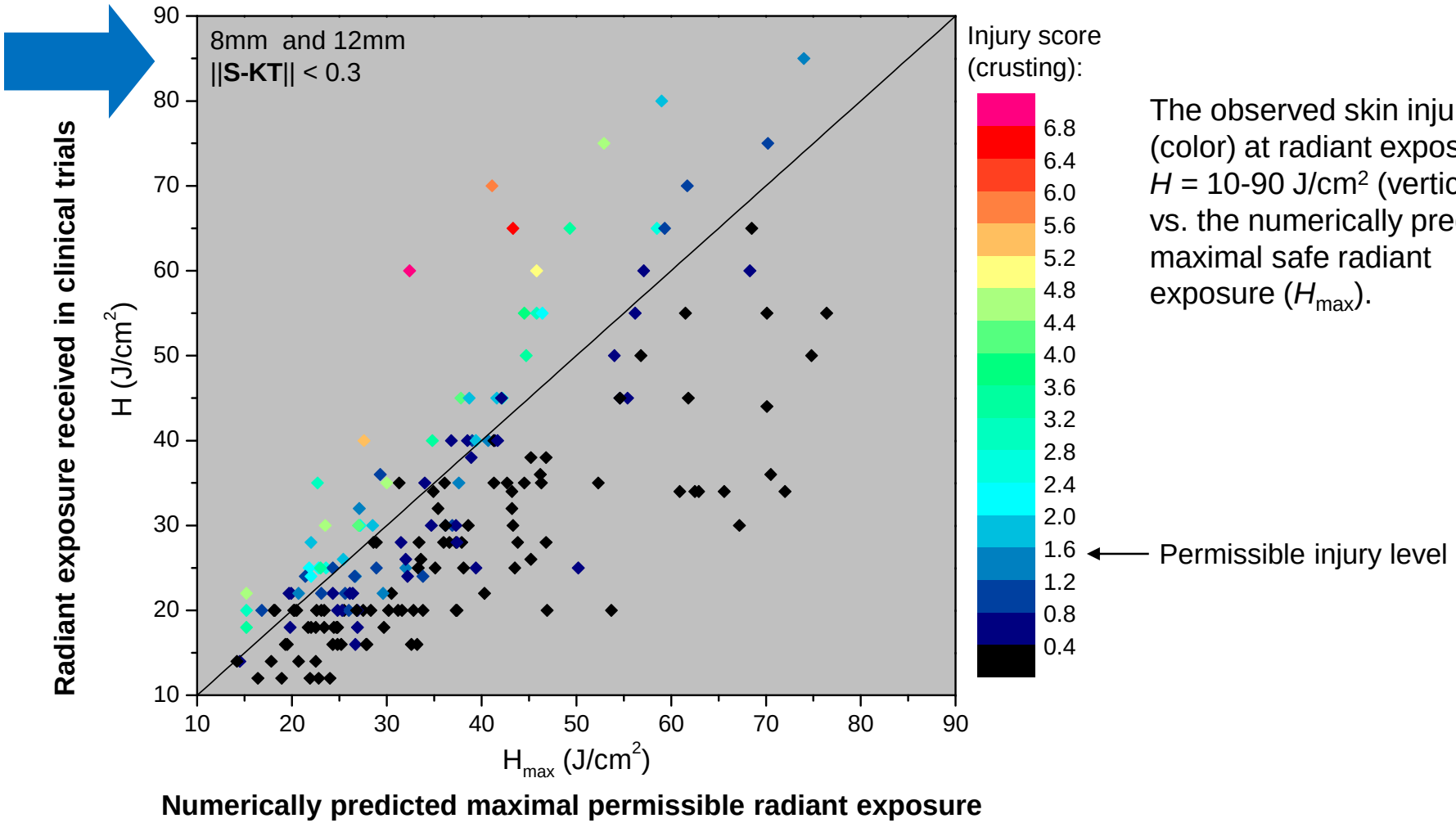

The observed skin injury (color) at radiant exposures H = 10-90 J/cm^2 (vertical) vs. the numerically predicted maximal safe radiant exposure (H_{max}).

All irradiations at radiant exposures H below the individually predicted H_{max} (diagonal line) resulted in negligible or minimal skin crusting (injury score < 2.0).

Majaron et al., Lasers Surg. Med. sup. 23, 916 (2011)

Summary 2 - Biomedical applications of PPTR profiling

PPTR combines high optical contrast with rather uniform heat transport in soft tissues.

PPTR temperature profiling can provide valuable structural information on selected cutaneous structures, lesions, etc. *in vivo* with sufficient accuracy and robustness for several relevant applications:

- depth of PWS vasculature
- monitoring of tatoo removal

In addition, it provides quantitative information on laser-induced temperature rise and thus a unique insight into light interaction with selected targets

- study of PWS response to laser treatment
- evaluation of a prototype laser system for skin rejuvenation (1342 nm)
- determination of individual safe radiant exposure
- ...

3. Beyond temperature profiling:

Model-based inverse analysis

- assessment of structure and composition of human skin
- quantitative analysis of hemoglobin dynamics in traumatic bruises
- combining PPTR and diffuse reflectance spectroscopy (DRS)

Optical model of healthy skin (2-layer)

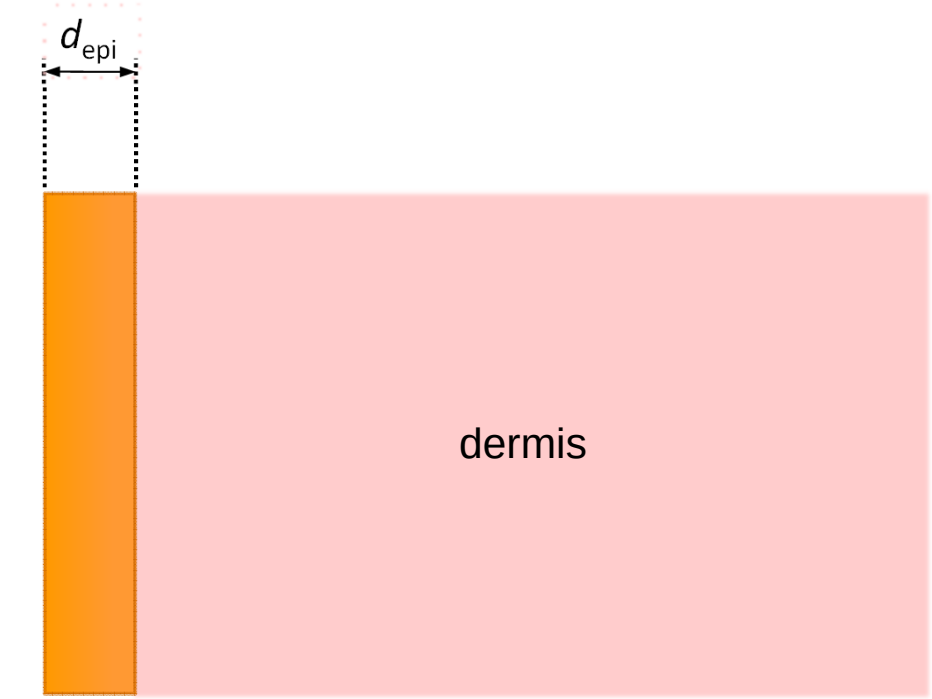

f_{mel}

f_{bl} , S_{bl}

Reduced scattering coefficient (epidermis and dermis):

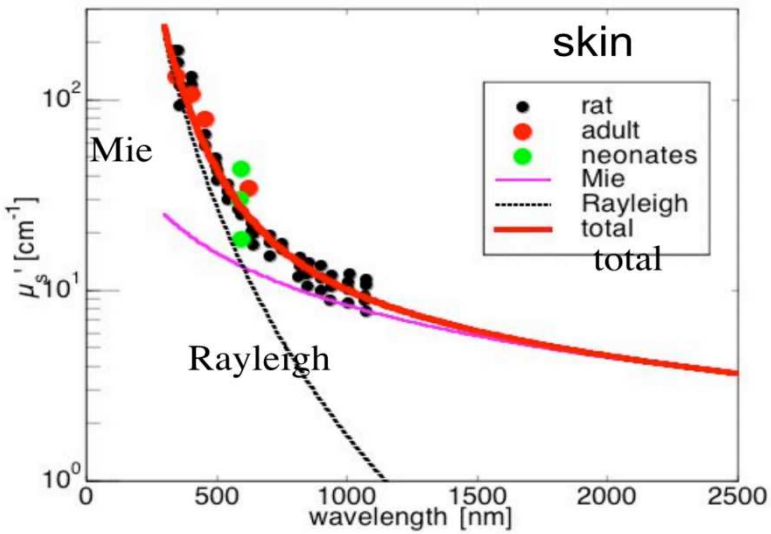

$$\mu_s'(\lambda) = a\left[f\left(\frac{\lambda}{500\ \mathrm{nm}}\right)^{-4} + (1-f)\left(\frac{\lambda}{500\ \mathrm{nm}}\right)^{-b}\right]$$

$$a = 43.8\ \mathrm{cm}^{-1},\ f = 0.46,\ \ b = 0.84$$

Jacques, J. Biophoton. 3, 75 (2010)

Determination of skin properties using PPTR

Intact skin parameters:

d_{epi} , f_{mel} , f_{bl} , S

Correct

(lsqnonlin)

Compare with measured ΔS(t)

~~Temperature profiling~~

MCML

(532 nm)

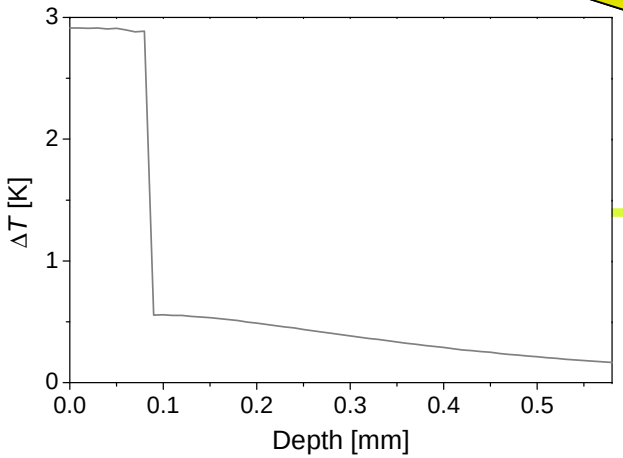

$$S = K\,T$$

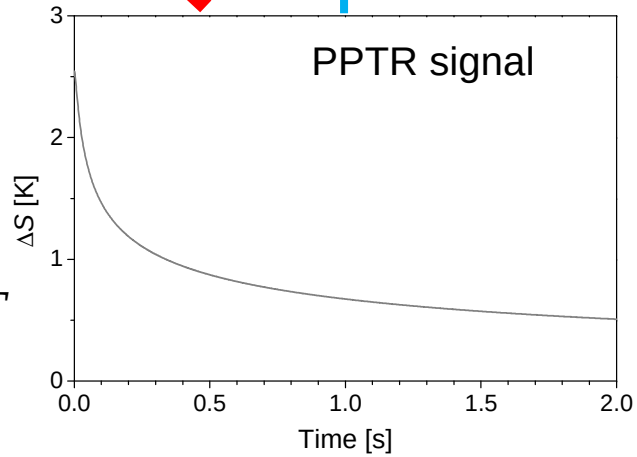

MCML =

Monte Carlo

for multiple layers *

- 10^7 photons per run
- parallelized for GPU (*CUDA*)

** Wang et al., Comput. Methods Programs Biomed. 47:131 (1995)*

Assesment of the healthy skin specifics

PPTR signals

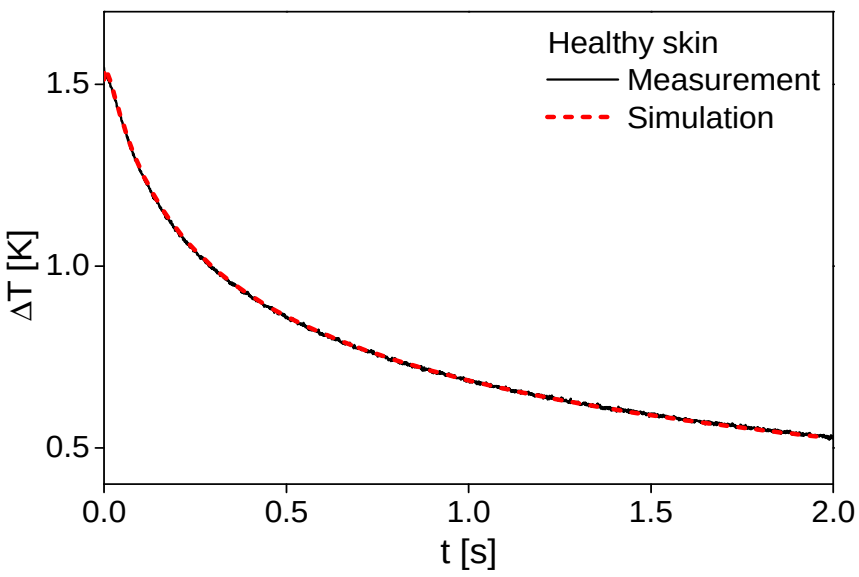

Temperature profiles

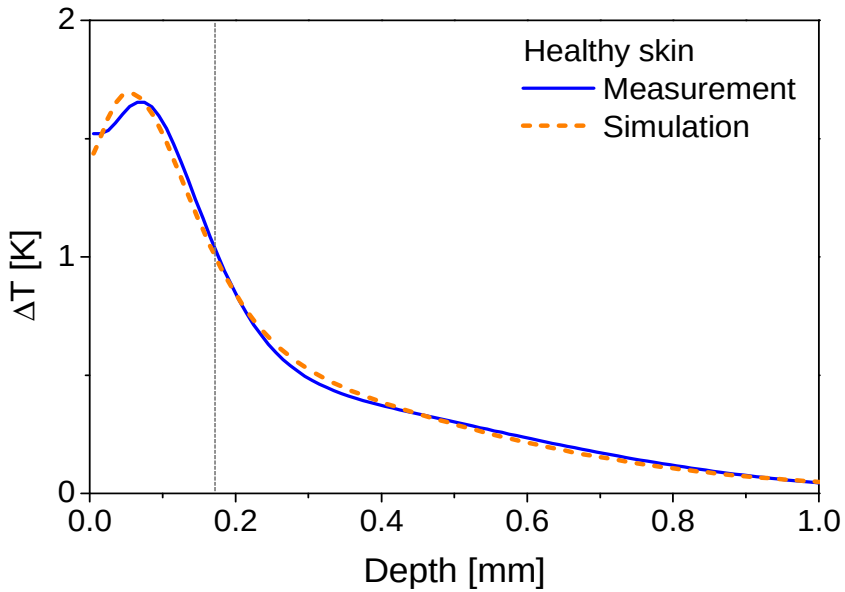

- epidermal thickness: d_{epi} = 0.17 mm
- melanin concetration: f_{mel} = 1.4 %
- blood concentration: f_{bl} = 2.7 %
- blood oxygenation: S = 80 % *(fixed)*

Vidovič et al., J. Biomed. Opt. 20, 017001 (2015)

Study of hemoglobin dynamics in traumatic bruises

t = 16 h | 43 h | 92 h | 115 h

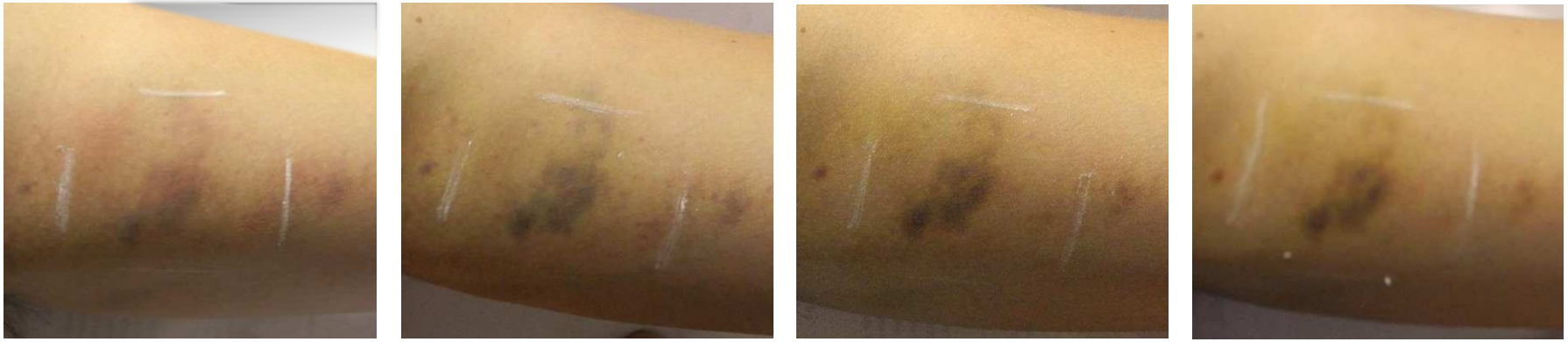

Motivation

Enable objective determination of the bruise age in forensic investigations

- currently based on subjective impression (the perceived color)
- inaccurate due to uncontrolled ambient lighting, skin thickness, pigmentation ...

Specific goal

Establish a mathematical model of the bruise dynamics

- assess the key parameter values in controlled experiments

Analytical model of the bruise dynamics

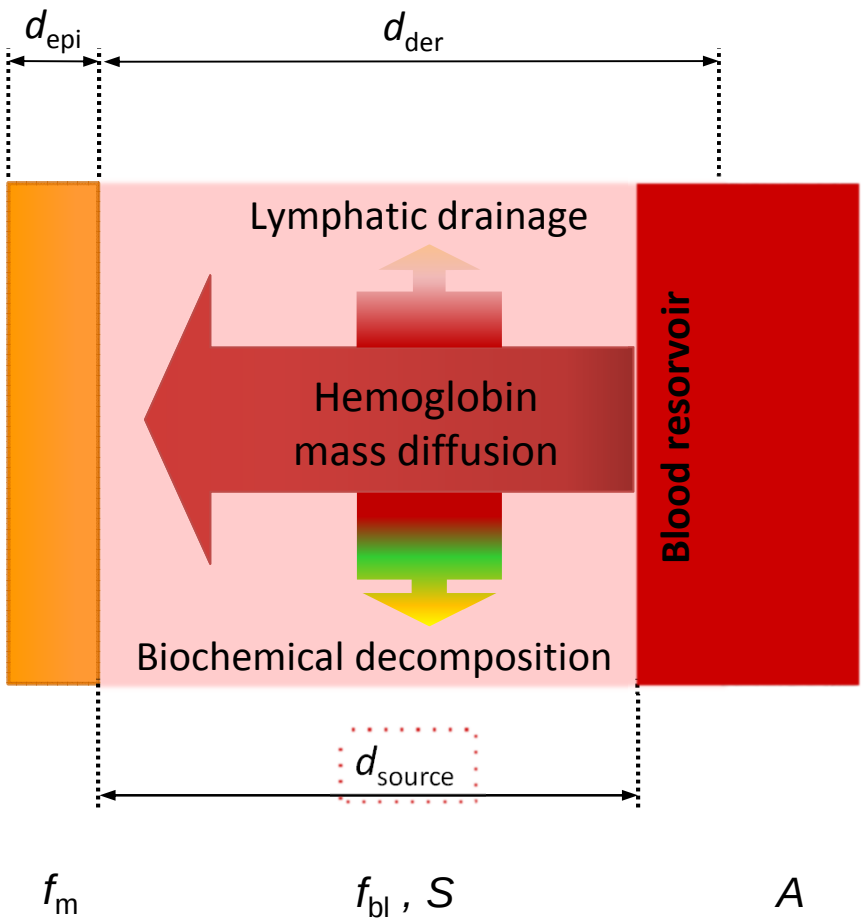

Hemoglobin concentration, $f_h(z,t)$:

$$\frac{\partial f_h}{\partial t} = D_h \nabla^2 f_h - \frac{f_h}{\tau_h}$$

D_h : mass diffusion coefficient

τ_h : lymphatic system drainage
+ conversion to biliverdin

Bilirubin concentration, $f_b(z,t)$:

$$\frac{\partial f_b}{\partial t} = \frac{f_h}{\tau_{bg}} - \frac{f_b}{\tau_{br}}$$

τ_{br} : bilirubin generation

τ_{br} : lymphatic system drainage
+ conversion to hemosiderin

Randeberg et al, Lasers Surg Med. 38, 277 (2006)

Temperature profiles induced in healthy vs. bruised skin

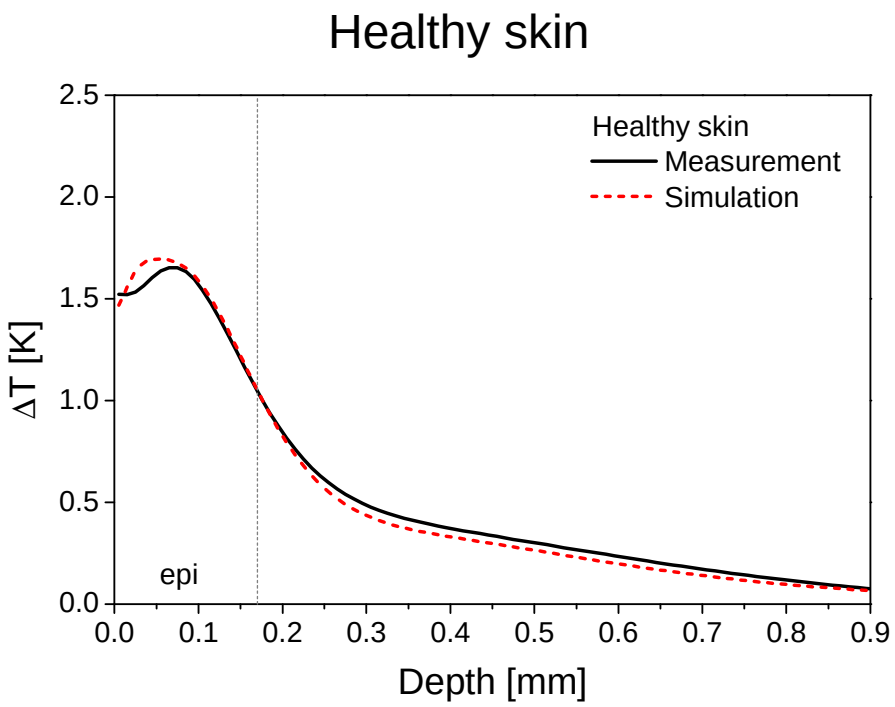

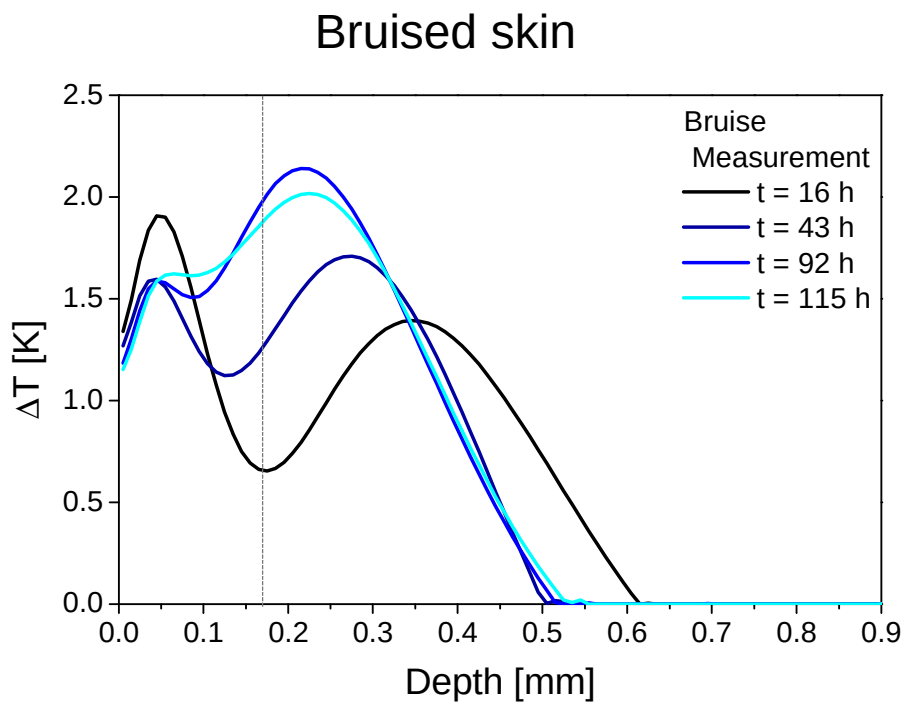

- epidermal thickness: d_{epi} = 0.17 mm
- melanin concetration: f_{mel} = 1.4 %
- blood concentration: f_{bl} = 2.7 %
- blood oxygenation: S = 80 % *(fixed)*

- Hb mass diffusivity
- Hb decomposition time
- source depth
- source time

Analysis of bruise dynamics using PPTR

Bruise model parameters:
D_h, τ_h, d_{source}, T

Correct
(lsqnonlin)

Compare with measured $\Delta S(t)$

Analit.

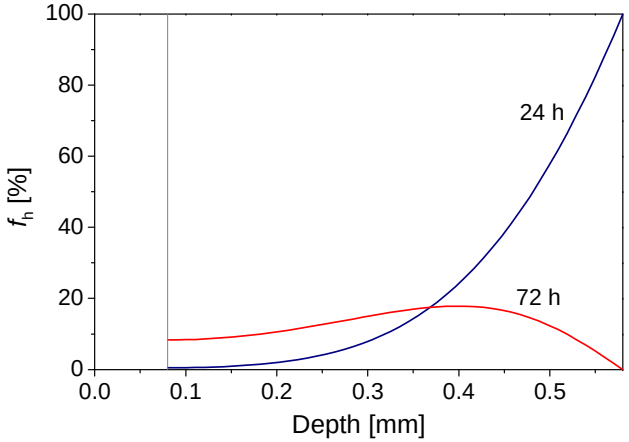

MCML
(532 nm)

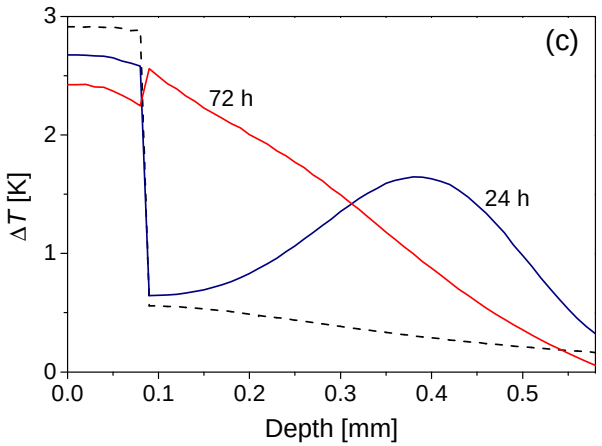

$$S = K\,T$$

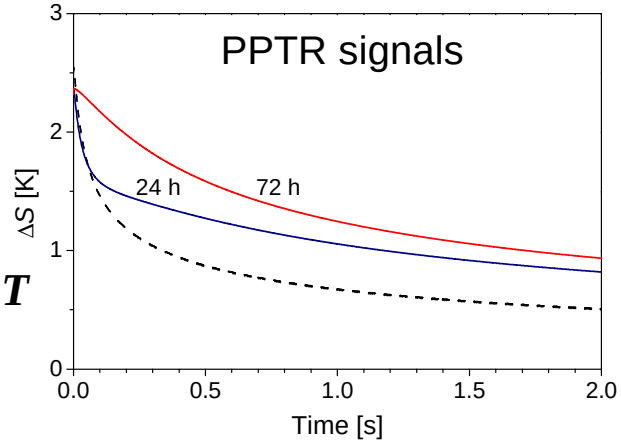

Bruised skin

t = 16 h

t = 92 h

PPTR signals:

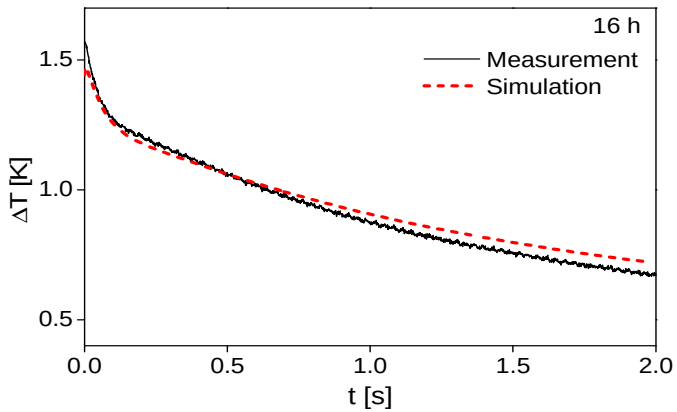

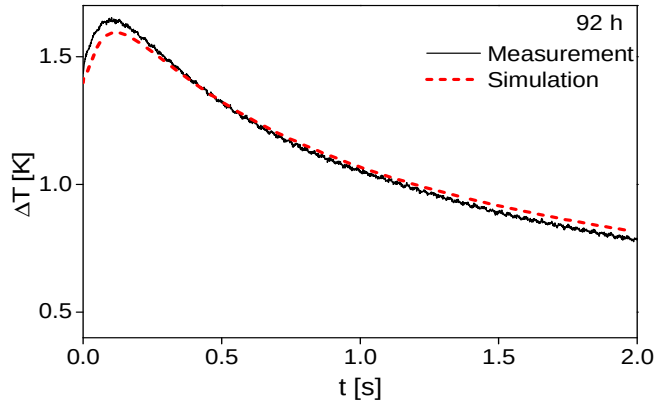

Temperature profiles:

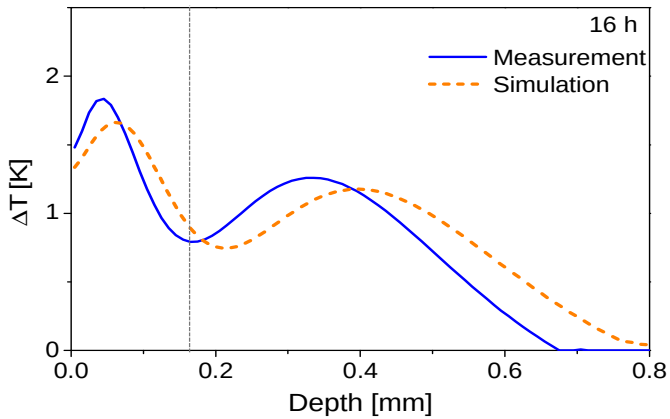

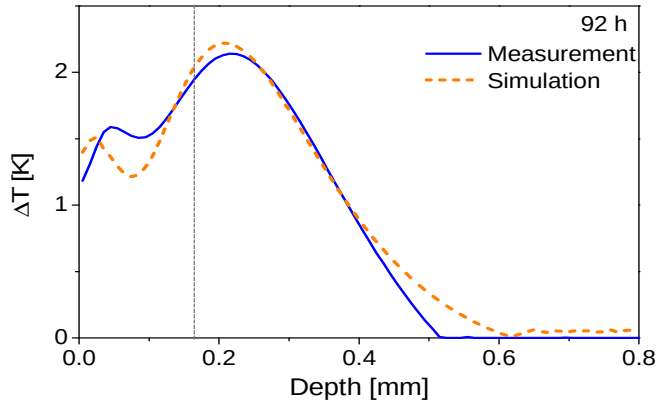

- d_{der} (mm) =
- D_h (10^{-4} mm^2/h) =
- τ_h (h) =
- T (h) =

t = 16 h	t = 92 h
0.47 ± 0.01	0.48 ± 0.01
6.6 ± 0.1	6.2 ± 0.2
51 ± 5	81 ± 3
> 16	38 ± 3

Vidovič et al., J. Biomed. Opt. (2015)

II. Temporally variable: τ

Constant: D, d_{der}, T

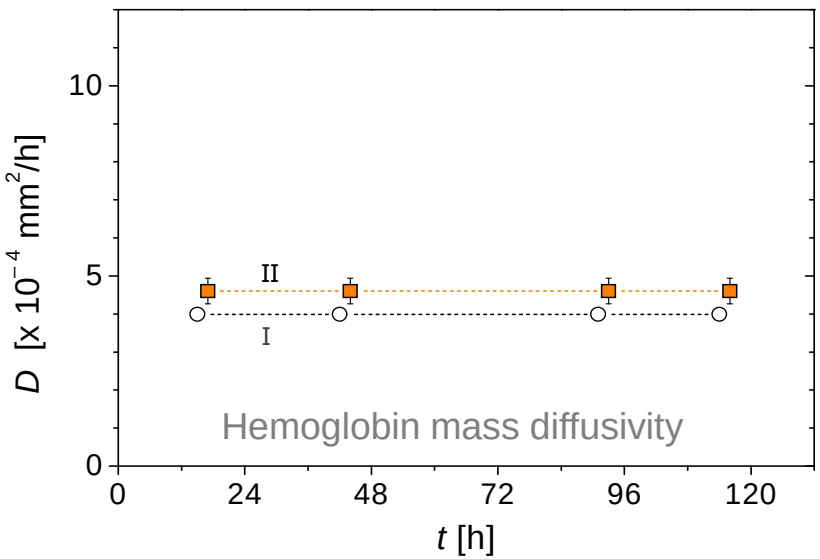

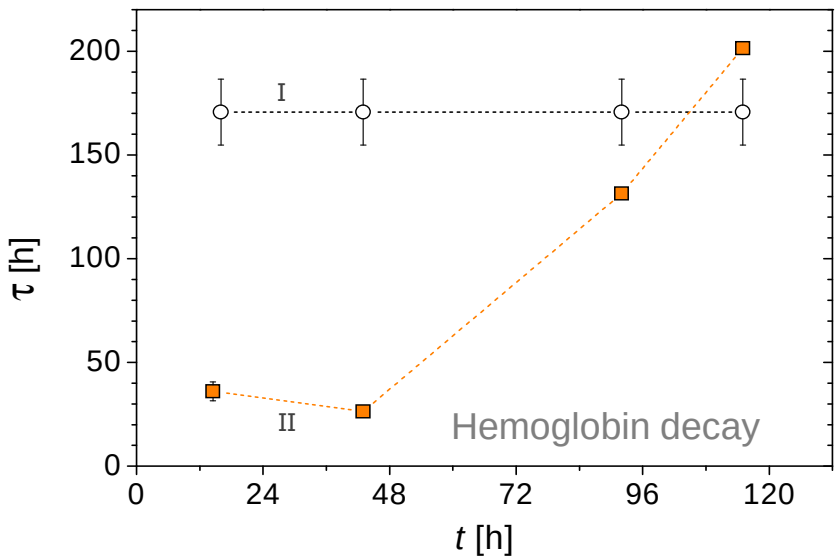

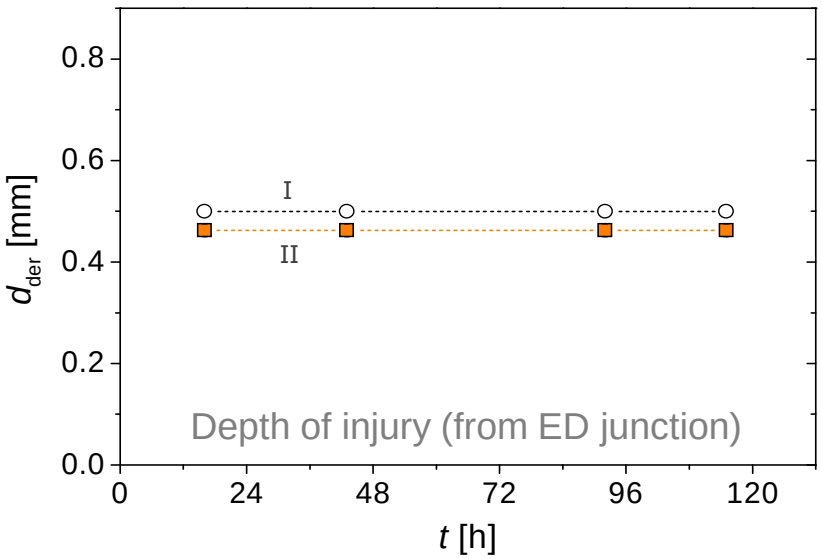

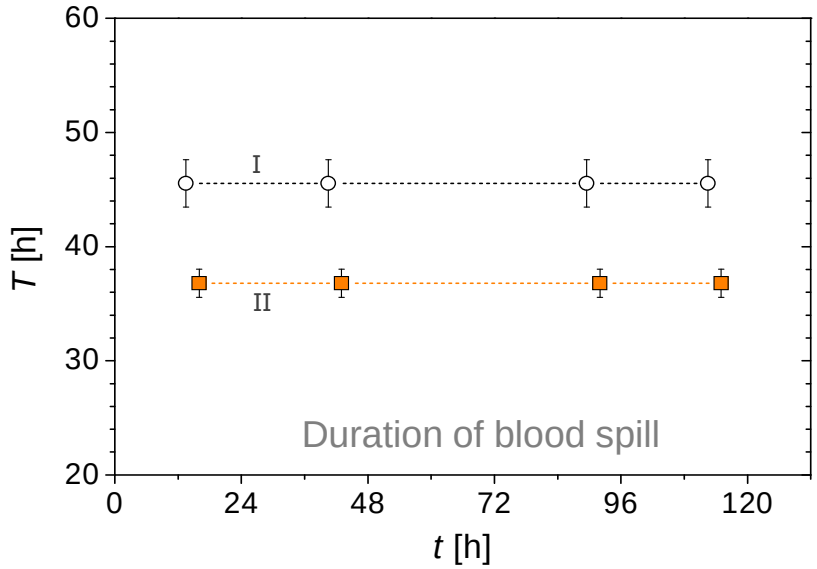

Vidovič et al., J. Biomed. Opt. 20, 017001 (2015)

Note: A nice fit does not guarantee that the results are accurate **!**

- monitor the correlations between the fitted variables !

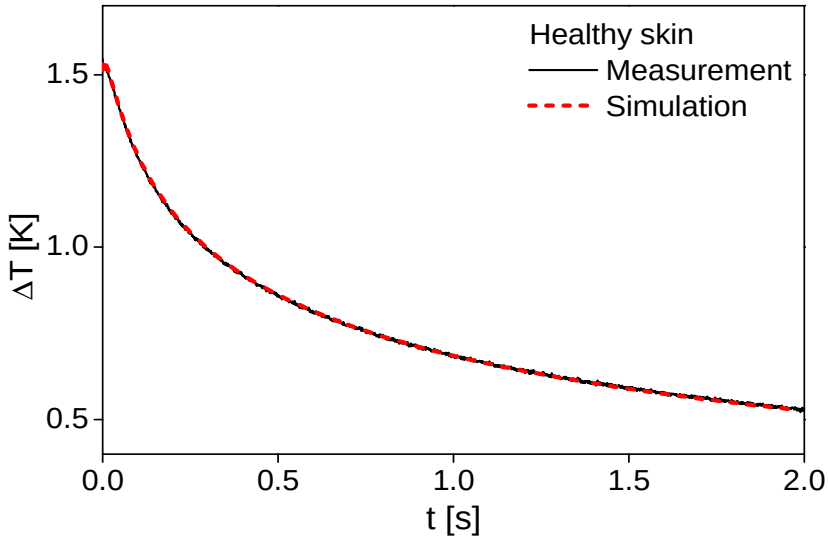

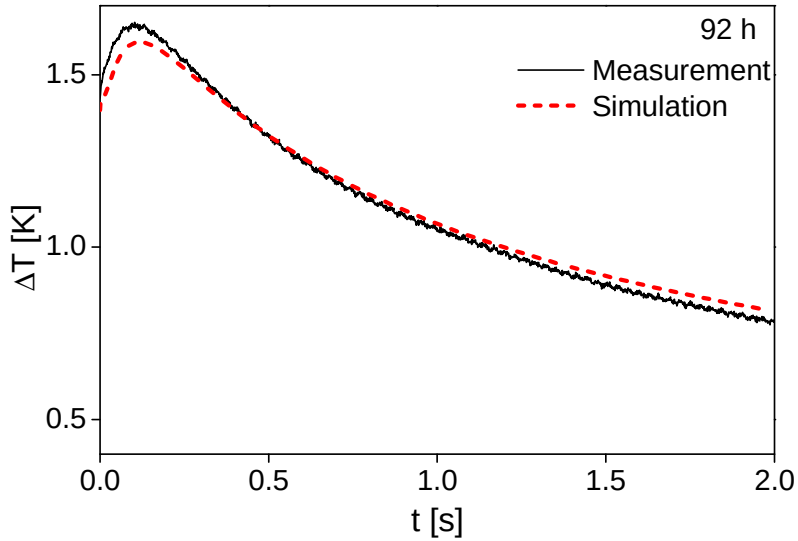

	d_{epi}	f_{mel}	f_{bl}
d_{epi}	1	−0.86	−0.91
f_{mel}	−0.86	1	0.62
f_{bl}	−0.91	0.62	1

	D	τ	d_{der}	T
D	1	−0.57	0.59	0.56
τ	−0.57	1	−0.72	−0.99
d_{der}	0.59	−0.72	1	0.63
T	0.56	−0.99	0.63	1

Vidovič et al., J. Biomed. Opt. 20, 017001 (2015)

Add: Diffuse Reflectance Spectroscopy (DRS)

<u>24 healthy volunteers</u> (so far)

- males and females
- age: 20–60 years
- skin phototypes: I–III
- known time of injury
- skin surface intact

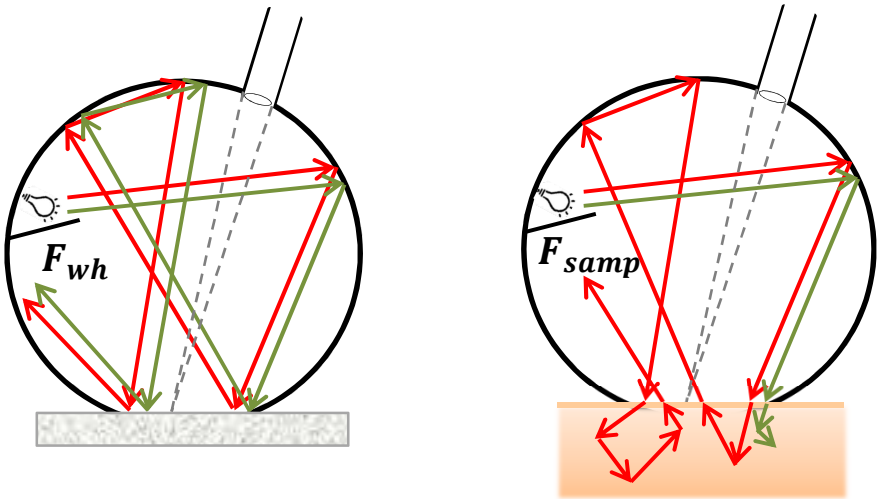

<u>DRS measurements</u>:

- integrating sphere (ISP-REF, Ocean Optics)
- λ = 400–650 nm (USB4000, Ocean Optics)
- correct raw DRS data for single-beam substitution error (SBSE)*

** Vidovič et al., J. Biomed. Opt. 19, 027006 (2014)*

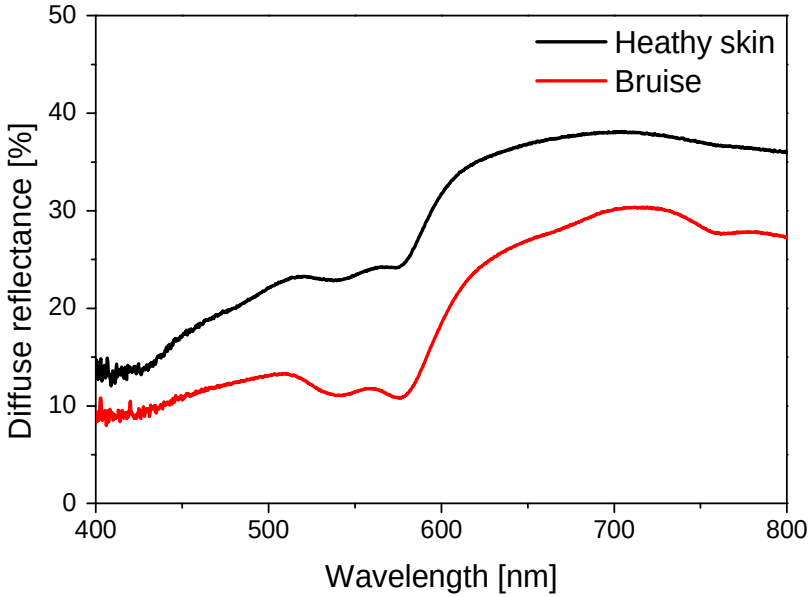

Vidovič et al., Proc. SPIE, 9540, 95400E (2015)

3-layer optical model of intact skin

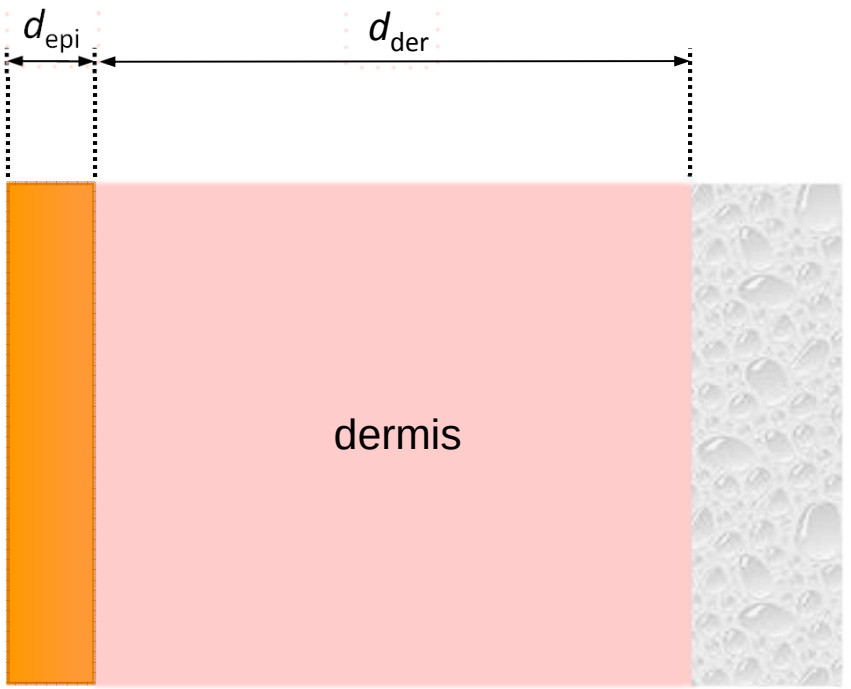

epidermis adipose

f_{mel}
$f_{bl,epi}$

f_{bl} , S_{bl}

A

Scattering in the adipose

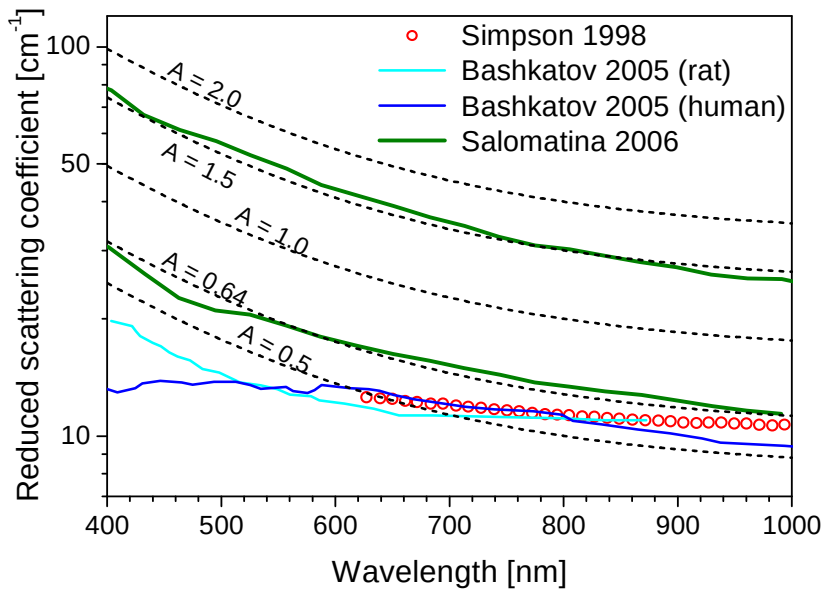

$$\mu'_{s,sub}(\lambda) = A\left[16.43\,\mathrm{cm}^{-1} + 303.8\,\mathrm{cm}^{-1}\exp\left(-\frac{\lambda}{180.3\,\mathrm{nm}}\right)\right]$$

$$0.5 \le A \le 2.0$$

Naglič et al., Proc. SPIE, 90320N (2013)

Characterization of intact skin by combined PPTR and DRS

Intact skin parameters:
d_{epi}, d_{der}, f_{mel}, $f_{bl,epi}$, f_{bl}, S, A

Correct
(lsqnonlin)

Compare with measured $R_d(\lambda)$ *and* $\Delta S(t)$

MCML
(12 x)

MCML
(*532 nm*)

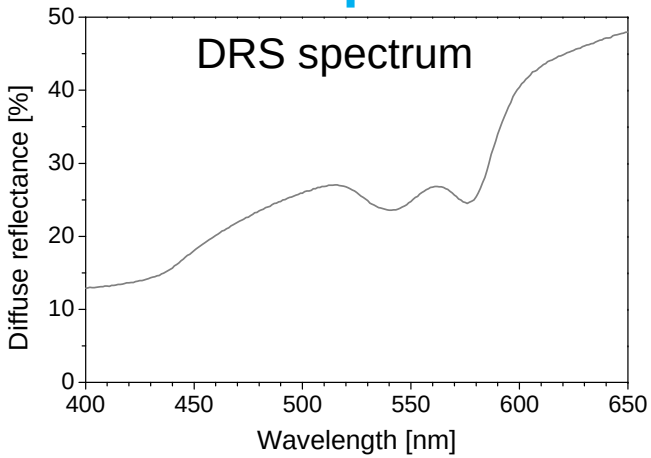

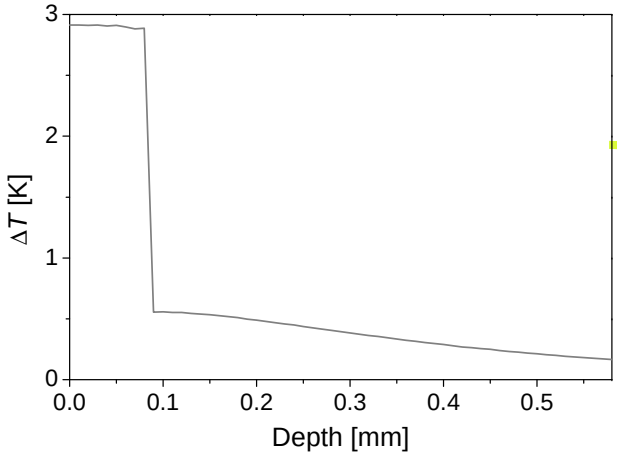

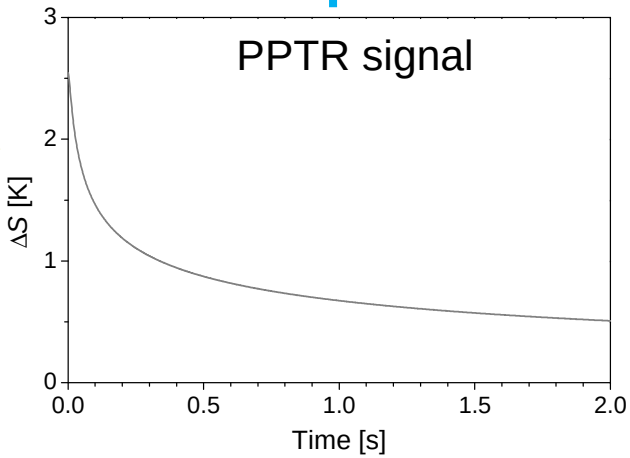

MCML =
Monte Carlo
for multiple layers *
- finite IS aperture
- 10^7 photons per wavel.
- GPU (*CUDA*)

** L. Wang, S. Jacques*

Parameters of intact skin - the combined PPTR/DRS approach

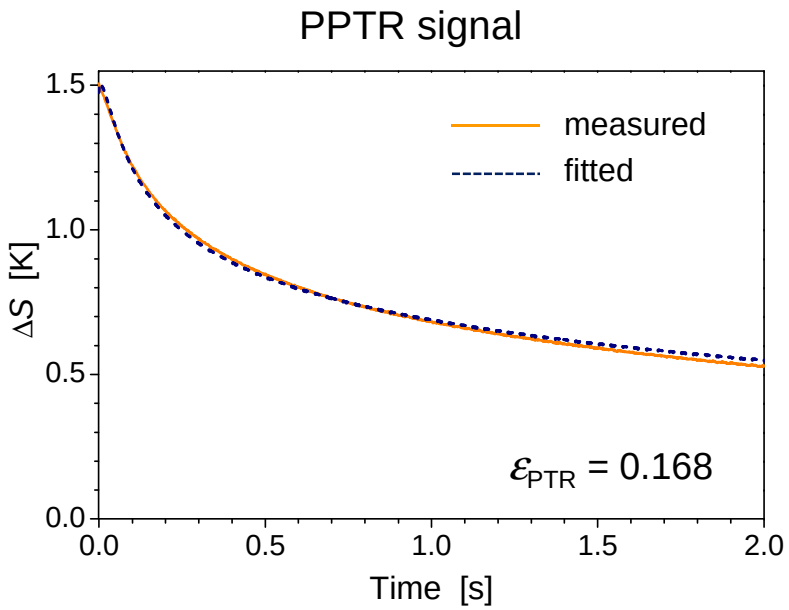

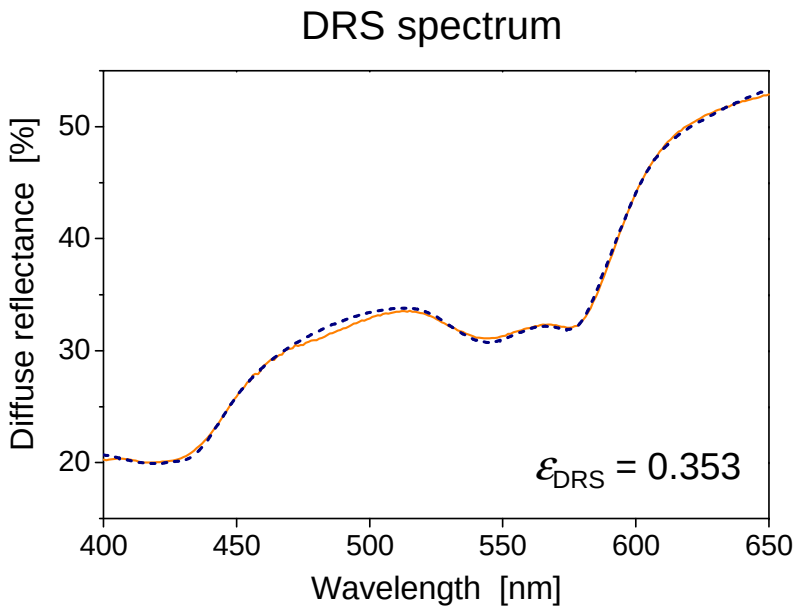

- epidermal thickness: d_{epi} = 0.16 mm
- dermal thickness: d_{der} = 0.88 mm
- melanin content: f_{mel} = 0.80 %
- epidermal blood content: $f_{bl,epi}$ = 0.2 %
- dermal blood content: f_{bl} = 1.37 %
- oxygen saturation: S = 38 %
- adipose scattering: A = 2.0

Increasing the dermal scattering amplitude (by 15%) improves the match !

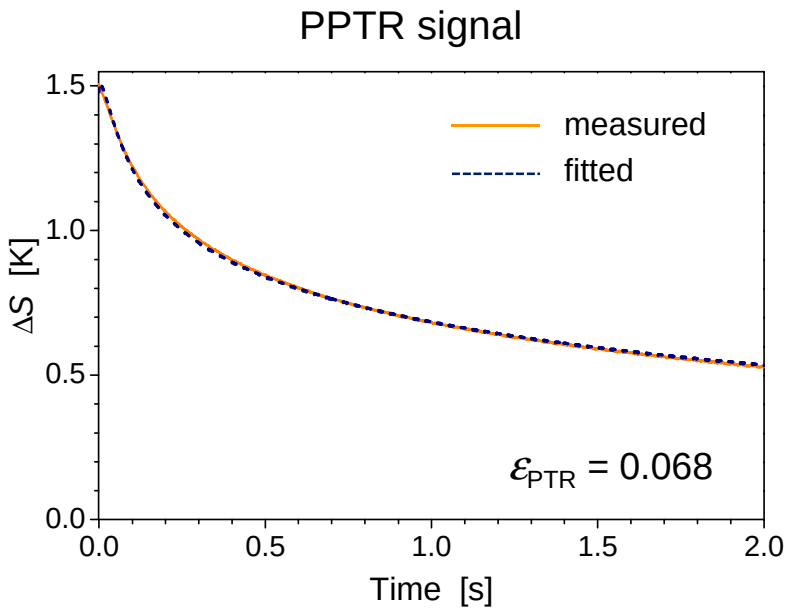

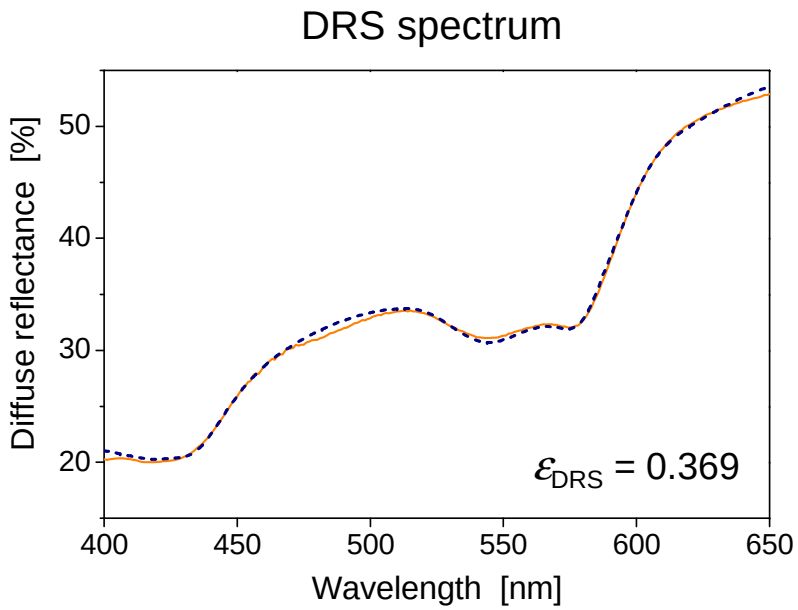

- epidermal thickness: d_{epi} = 0.15 mm
- dermal thickness: d_{der} = 0.66 mm
- melanin content: f_{mel} = 0.9 %
- epidermal blood content: $f_{bl,epi}$ = 0.2 %
- dermal blood content: f_{bl} = 1.7 %
- oxygen saturation: S = 37 %
- adipose scattering: A = 1.7

Nina Verdel et al., Poster P.13 (2016)

Bruise evolution timeline

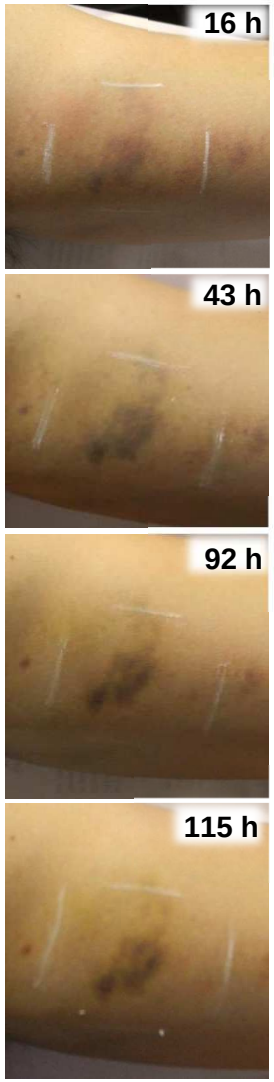

man, 27 y. (AK_15)

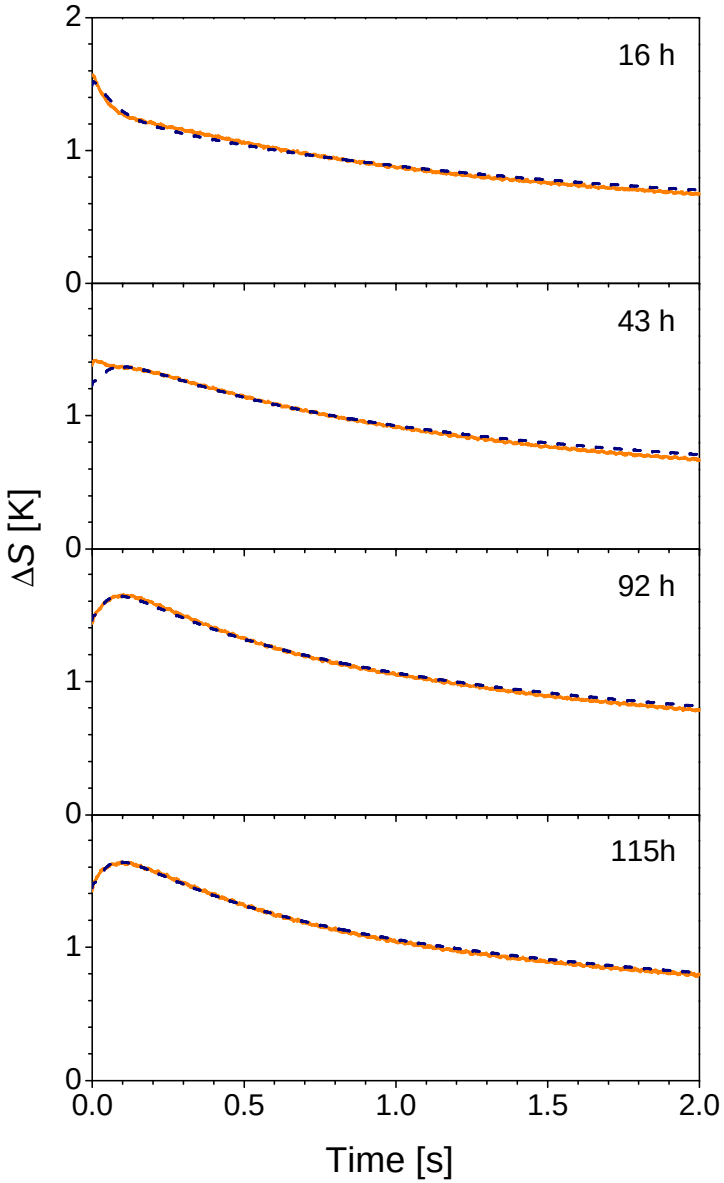

measured

fitted

- Hb mass diffusivity:

  $D_h = (8.6 \pm 0.3) \times 10^{-4}$ mm²/h

- Hb decomposition time:

  $\tau = (121 \pm 8)$ h

- source depth:

  $d_{source} = (0.54 \pm 0.01)$ mm

- source time:

  $T = (50 \pm 1)$ h

Marin et al., Laser Surg. Med. sup 27 (2016)

Bruise evolution timeline

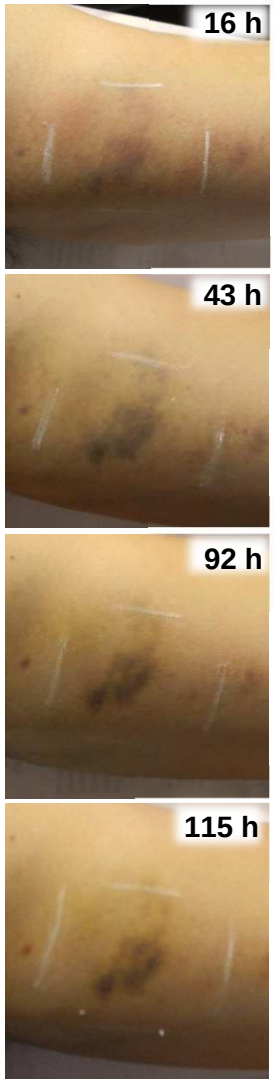

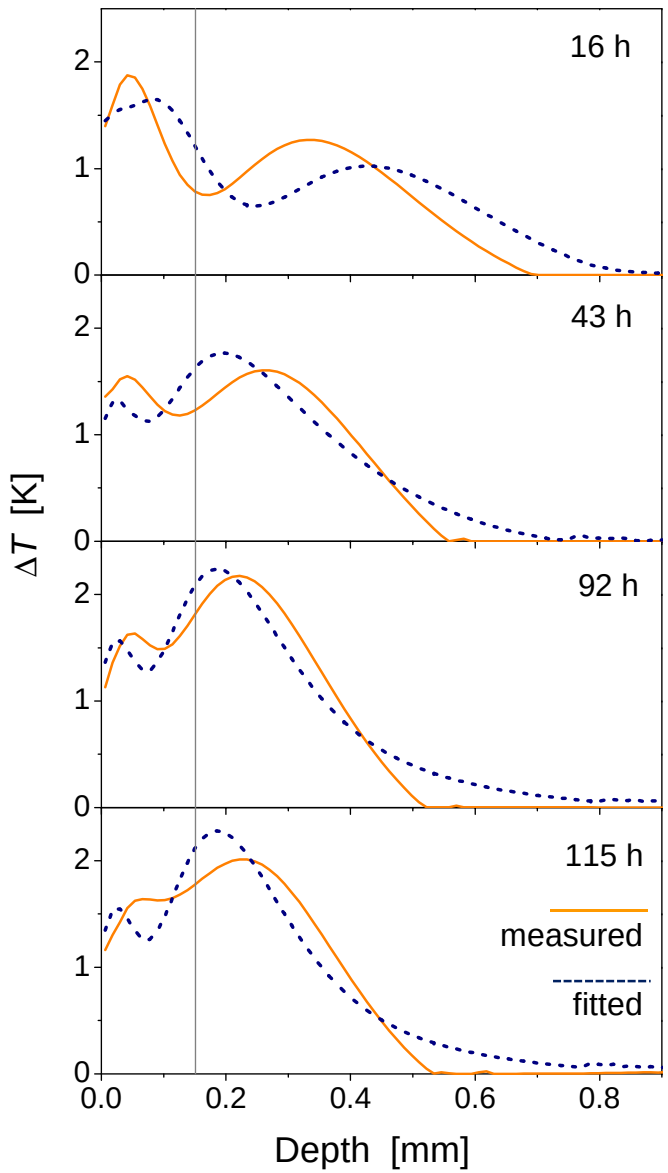

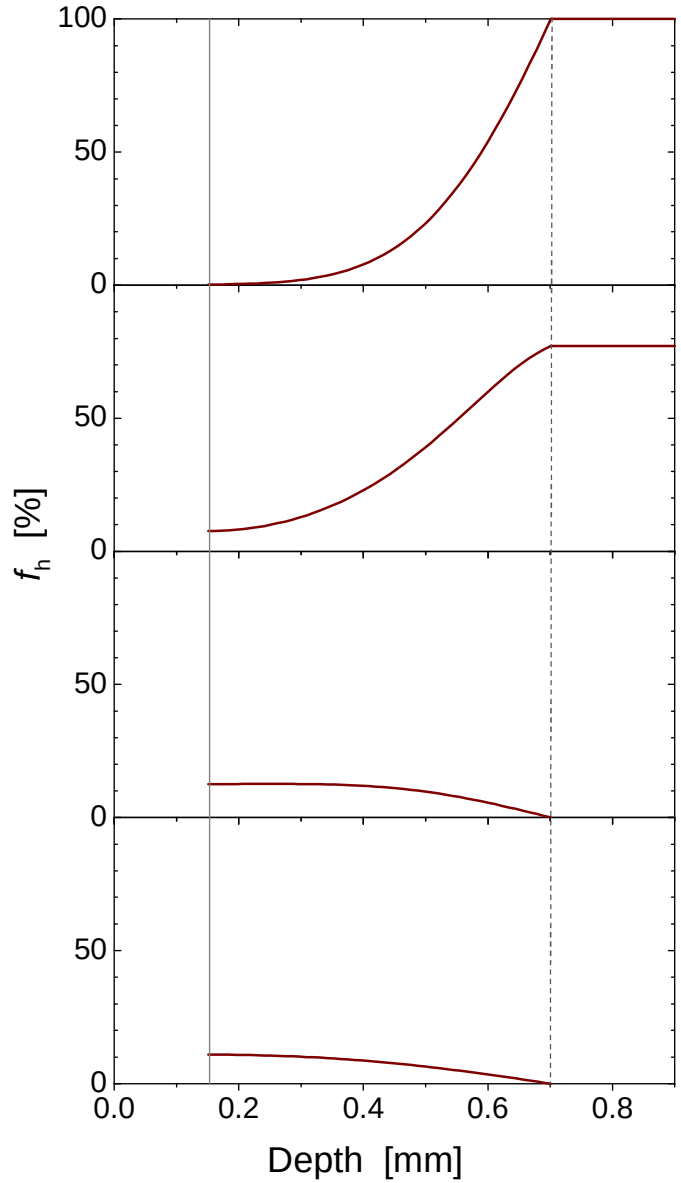

man, 27 y. (AK_15)

Analysis of bruise dynamics by combined PPTR and DRS

Bruise model parameters:
D_h, τ_h, S_h, τ_{bg}, τ_{br}, d_{source}, T

Correct
(lsqnonlin)

Compare with measured $\Delta S(t)$ and $R_d(\lambda)$

Analit.

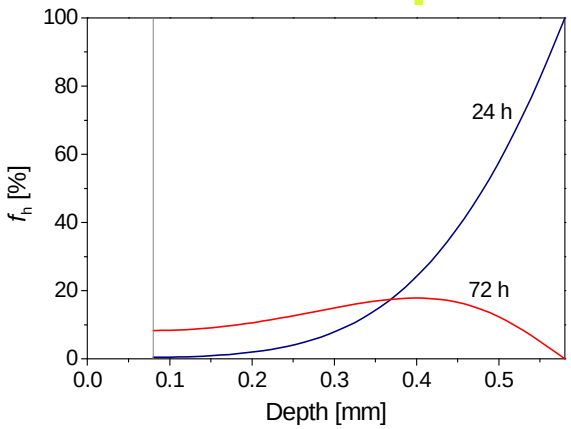

MCML

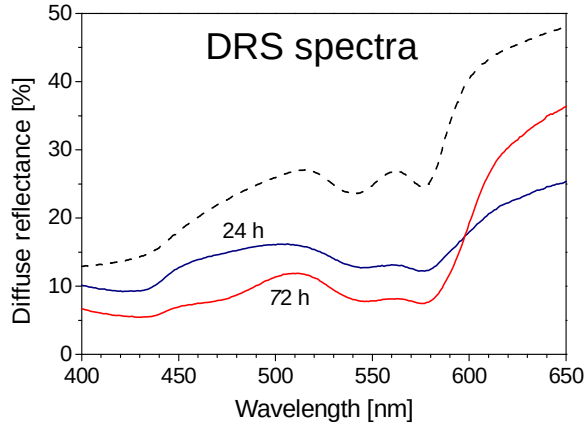

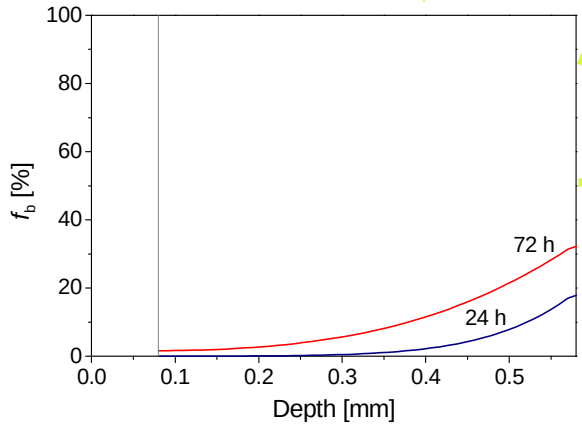

MCML

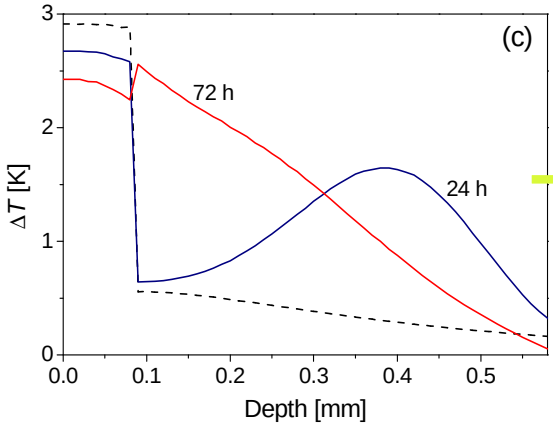

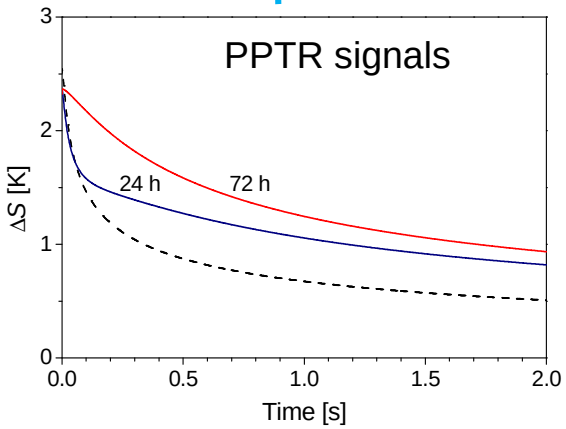

II. Allow to vary with time: τ_h, d_{der}, S_h, τ_{bg}

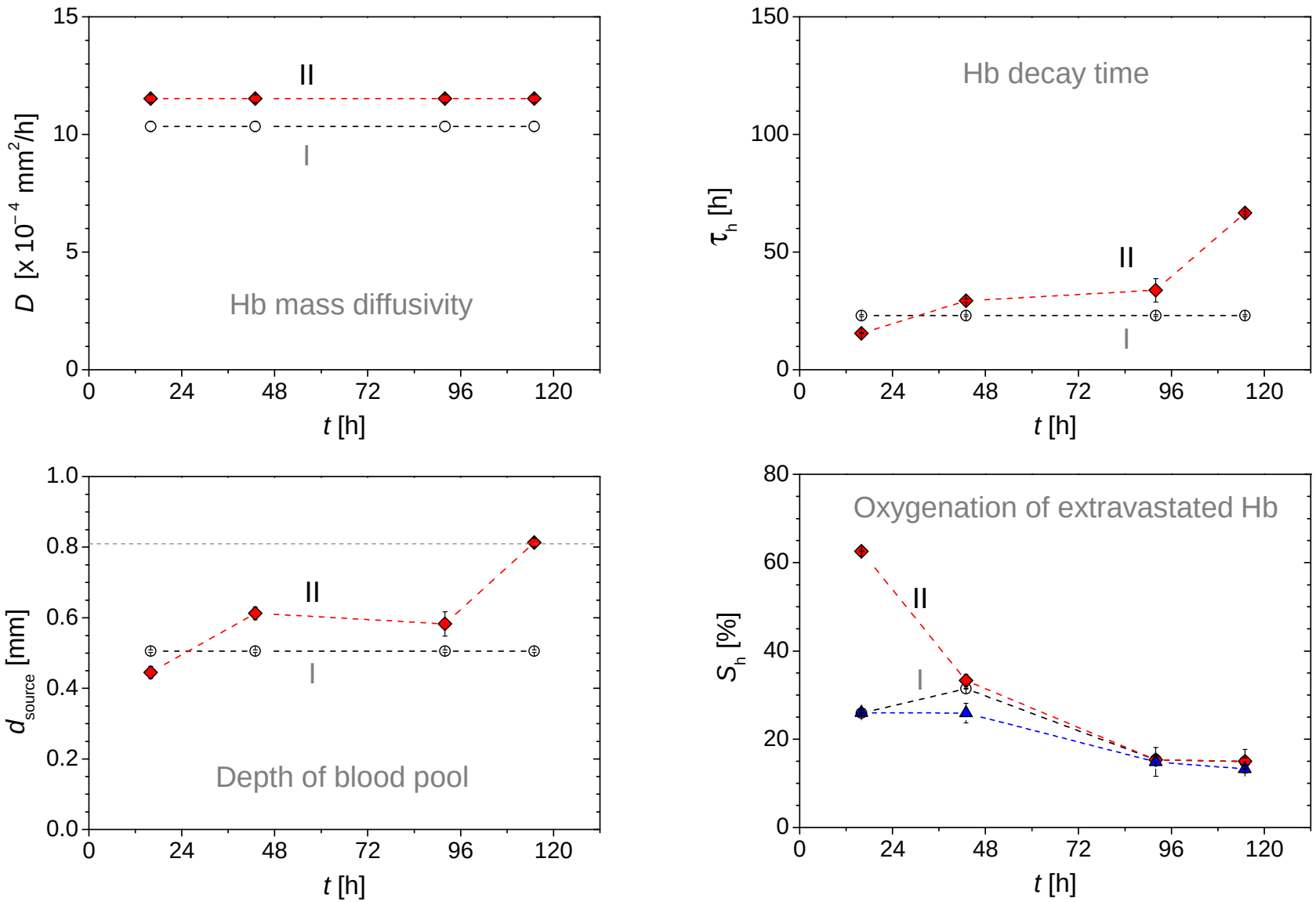

Vidovič et al., Proc. SPIE, 95400E (2015)

Example #2: Twin bruises

Left knee:

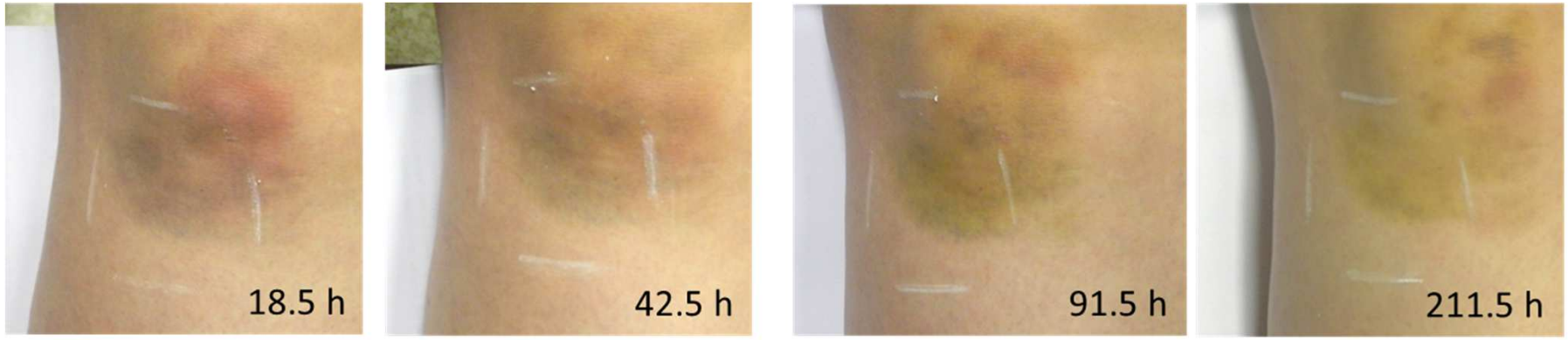

Right knee:

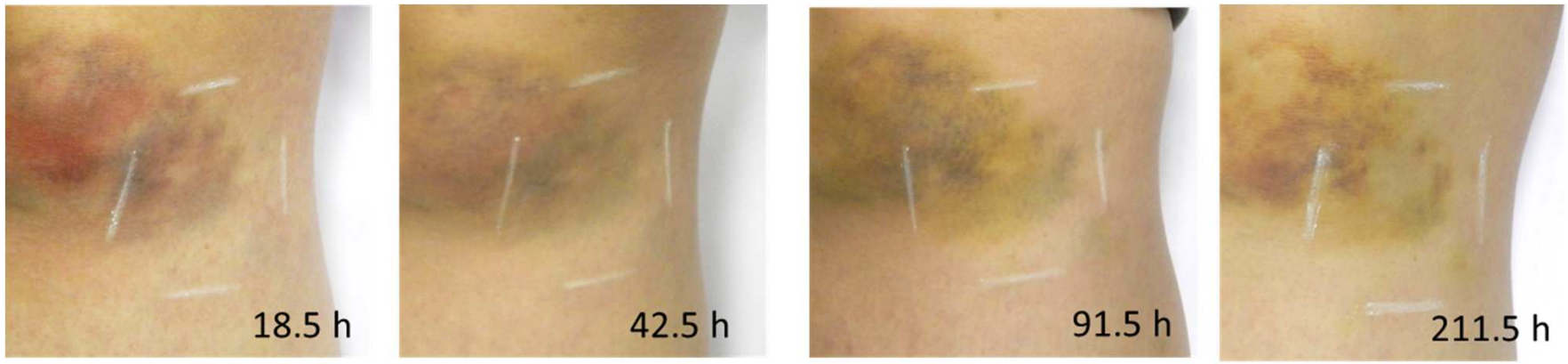

women, 29 y. (ER_12, ER_13)

Twin bruises: results

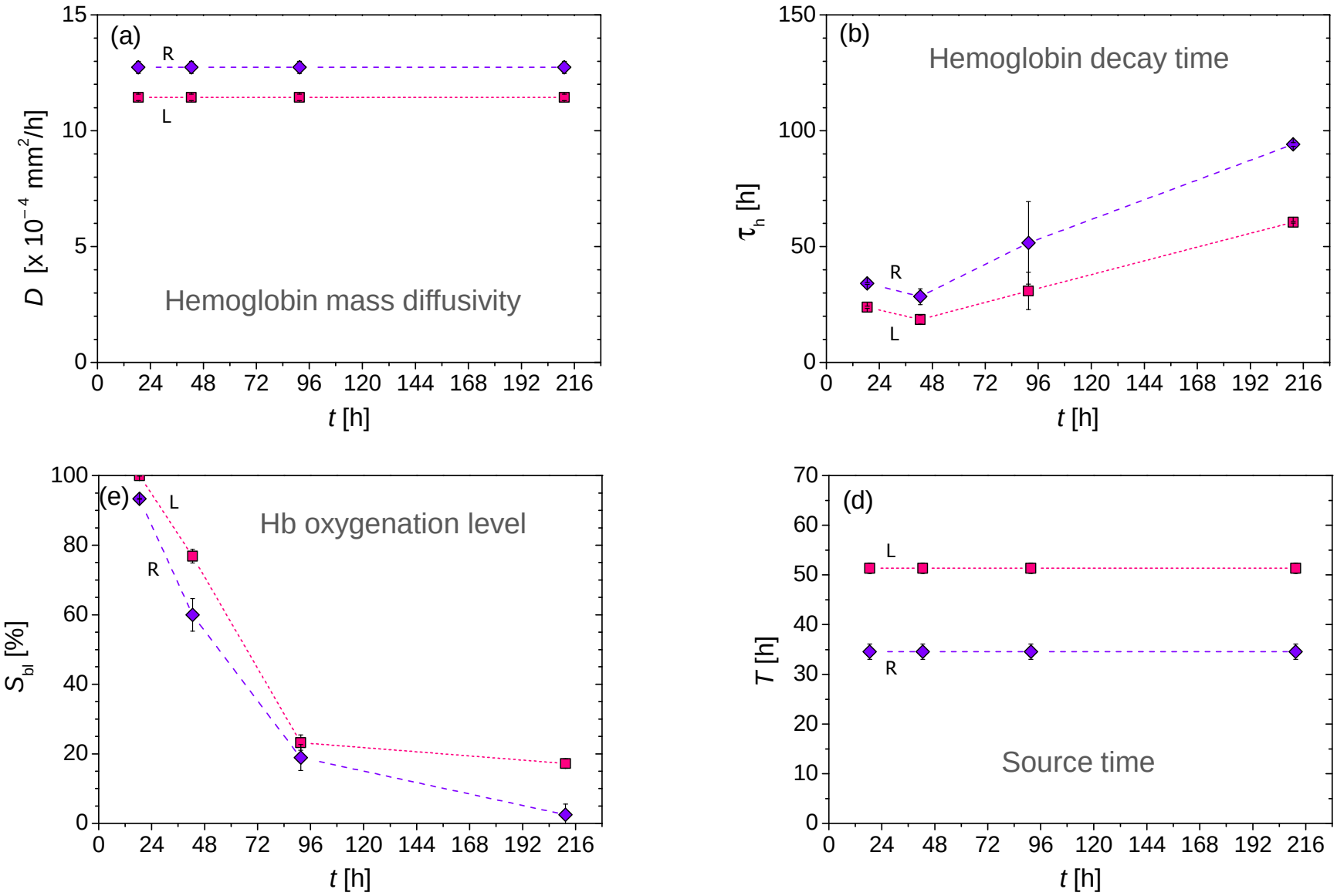

Vidovič et al., Proc. SPIE, 95400E (2015)

Summary 3 - Model-based inverse analysis

Model-based analysis reduces ill-posedness of the inverse problem

- by limiting the number of free variables, and
- constraining them by applying prior knowledge

This enables noninvasive assessment of skin structure and composition

- using numerical modeling of light transport in tissue (inverse Monte Carlo)

Combining PPTR with DRS improves the robustnes of inverse analysis

- epidermal and dermal thickness, melanin content, blood content, oxygenation ...

The approach is amenable to analysis of intra- and inter-patient variations, characterization of cutaneous lesions, etc.

- Hb dynamics in traumatic bruises (mass diffusion, decompostition time ...)
- assessment of both absorption and scattering properties might be possible *

**** Nina Verdel et al., Poster P.13 (2016)***

J. Stuart Nelson

Beckman Laser Institute & Medical Clinic
University of California at Irvine

Wim Verkruysse *(Philips Research, Eindhoven, Netherlands)*

Bernard Choi *(Beckman Laser Institute, Dept. of Biomedical Engineering; UC Irvine)*

Bincheng Li *(Institute of Optics and Electronics, CAS, Shuangliu, China)*

Matija Milanič, Luka Vidovič,*

Ana Marin, Nina Verdel

Jožef Stefan Institute,
Ljubljana, Slovenia

Faculty of Mathematics and Physics,
University of Ljubljana, Slovenia

** Analysis and Research Center, Bank of Slovenia*